

LOCAL DISCONTINUOUS GALERKIN METHODS WITH IMPLICIT-EXPLICIT TIME-MARCHING FOR TIME-DEPENDENT INCOMPRESSIBLE FLUID FLOW

HAIJIN WANG, YUNXIAN LIU, QIANG ZHANG, AND CHI-WANG SHU

ABSTRACT. The main purpose of this paper is to study the stability and error estimates of the local discontinuous Galerkin (LDG) methods coupled with multi-step implicit-explicit (IMEX) time discretization schemes, for solving time-dependent incompressible fluid flows. We will give theoretical analysis for the Oseen equation, and assess the performance of the schemes for incompressible Navier-Stokes equations numerically. For the Oseen equation, using first order IMEX time discretization as an example, we show that the IMEX-LDG scheme is unconditionally stable for \mathcal{Q}_k elements on cartesian meshes, in the sense that the time-step τ is only required to be bounded from above by a positive constant independent of the spatial mesh size h . Furthermore, by the aid of the *Stokes projection* and an elaborate energy analysis, we obtain the $L^\infty(L^2)$ optimal error estimates for both the velocity and the stress (gradient of velocity), in both space and time. By the *inf-sup* argument, we also obtain the $L^\infty(L^2)$ optimal error estimates for the pressure. Numerical experiments are given to validate our main results.

1. INTRODUCTION

In this paper we study a fully-discrete local discontinuous Galerkin (LDG) scheme coupled with multi-step implicit-explicit (IMEX) time discretization, for solving the following Oseen equation

$$(1.1) \quad \begin{cases} \frac{\partial \mathbf{u}}{\partial t} - \nu \Delta \mathbf{u} + \nabla \cdot (\boldsymbol{\gamma} \otimes \mathbf{u}) + \nabla p = \mathbf{f}, \\ \nabla \cdot \mathbf{u} = 0, \\ \mathbf{u}(\mathbf{x}, 0) = \mathbf{u}^0(\mathbf{x}) \end{cases}$$

in $\Omega \subset \mathbb{R}^2$. Here $\mathbf{x} = (x, y)$, ν is the kinematic viscosity, $\mathbf{u} = (u_1, u_2)$ is the velocity, $\boldsymbol{\gamma} = (\gamma_1, \gamma_2)$ is a given convective velocity field, p is the pressure, and $\mathbf{f} = (f_1, f_2)$ is the source term. Since p is uniquely defined up to an additive constant, we also assume that $\int_{\Omega} p \, dx dy = 0$. For the simplicity of analysis, we consider periodic boundary conditions, and assume $\mathbf{f} = \mathbf{0}$ in this paper, and without loss of generality, we assume γ_1 and γ_2 are positive.

Received by the editor October 23, 2016, and, in revised form, June 15, 2017 and July 1, 2017.
 2010 *Mathematics Subject Classification*. Primary 65M12, 65M15, 65M60.

Key words and phrases. Local discontinuous Galerkin method, implicit-explicit scheme, incompressible flow, Oseen equation, Navier-Stokes, stability, error estimate.

The first author's research was sponsored by NSFC grant 11601241, Natural Science Foundation of Jiangsu Province grant BK20160877, and NUPTSF grant NY215067.

The second author's research was sponsored by NSFC grant 11471194.

The third author's research was supported by NSFC grants 11671199, 11571290, and 11271187.

The fourth author's research was supported by DOE grant DE-FG02-08ER25863 and NSF grant DMS-1418750.

The LDG method was introduced by Cockburn and Shu [9] for convection-diffusion problems, motivated by the work of Bassi and Rebay [2] for compressible Navier-Stokes equations. As an extension of discontinuous Galerkin (DG) schemes for hyperbolic conservation laws [10], the LDG scheme can easily handle meshes with hanging nodes, elements of general shapes and local spaces of different types, thus it is flexible for hp -adaptivity. Furthermore, the LDG methods enforce the conservation laws locally and in a conservative way, and it performs well for problems with shocks, steep gradients, or boundary layers. Owing to these advantages, LDG methods have been designed to solve incompressible fluid flows, such as the Stokes system [7], the Oseen equation [6] and Navier-Stokes equations [8]. However, all these works are for the steady problems. As far as the authors know, only a few works have been done on LDG methods for time-dependent incompressible flows. Recently, Wang et al. [19] adopted the characteristic local discontinuous Galerkin methods for time-dependent incompressible Navier-Stokes problems, they used the characteristic method to deal with the time derivative term and the nonlinear convection term together, and discretized the remaining terms by the LDG spatial discretization. The unconditional stability of the first order scheme was presented, but the error analysis was absent.

In [16–18], several Runge-Kutta type implicit-explicit (IMEX) time marching schemes [1] coupled with the LDG spatial discretization for solving one and two dimensional convection-diffusion problems have been studied, where the corresponding IMEX-LDG schemes have shown good stability and accuracy. These schemes have also been applied to the drift-diffusion model of semi-conductor devices in [14]. The advantages of IMEX schemes lie in that: it cannot only overcome the severe time step restriction, compared with the pure explicit time discretization schemes, but also obtain an elliptic-type algebraic system, which is easy to solve efficiently by many standard iterative methods. In this paper, we would like to study the stability and accuracy of the IMEX-LDG schemes for solving the time-dependent Oseen equations, where the convection term is treated explicitly, and both the viscosity term and the pressure term are treated implicitly. Since the LDG discretization for the Stokes system results in a differential algebraic equation (DAE) [13] with index 2, Runge-Kutta time discretization might reduce the order of accuracy in time for pressure, hence we consider multi-step IMEX time discretizations, which are developed in [12].

In our LDG schemes, we adopt the equal order polynomials for the velocity, the stress (gradient of velocity) and the pressure. We will prove that for the Oseen equations, the corresponding IMEX-LDG schemes are unconditionally stable for \mathcal{Q}_k elements on cartesian meshes, in the sense that the time-step τ is only required to be bounded from above by a positive constant independent of the spatial mesh size h . Furthermore, by the aid of the so-called *Stokes projection* and an elaborate energy analysis, we obtain the $L^\infty(L^2)$ optimal error estimates for both the velocity and the stress, in both space and time. We also obtain the optimal error estimates for the pressure in the $L^\infty(L^2)$ norm, by the *inf-sup* argument and an optimal estimate for the time difference of velocity. These results, especially the optimal error estimates for pressure, constitute the main highlight of this paper. Since the proof is quite technical, we only take the first order scheme (i.e., forward Euler in the explicit discretization and backward Euler in the implicit discretization) as an example to show the idea.

Another important contribution of this paper lies in that, it is the first time that the so-called *Stokes projection* associated with the LDG spatial discretization is studied and adopted to obtain the optimal error estimate, which will consequentially provide a powerful tool in the analysis for Navier-Stokes problems. Furthermore, it is worth mentioning that, the numerical flux we consider for the viscosity term and the pressure term are the classical “alternating” fluxes without any extra penalty terms, this is different from [3, 6, 19], where penalty terms are added to enhance the stability of the scheme. Finally, we point out that, our long-term goal is to study IMEX-LDG methods for the incompressible Navier-Stokes equations, the analysis of the Oseen problem is just an intermediate step.

The paper is organized as follows. In Section 2 we present the semi-discrete LDG schemes for the Oseen equation, and give some properties of the LDG schemes. We will focus on the study of the Stokes projection in Section 3, which plays an important role in obtaining the optimal error estimates. Sections 4 and 5 are devoted to the stability and error analysis of the first order fully-discrete IMEX-LDG methods, respectively. In Section 6 we will present numerical results to verify our results. The concluding remarks and a few technical proofs are given in Section 7 and the Appendix, respectively.

2. THE SEMI-DISCRETE LDG SCHEME AND ITS PROPERTIES

Let $\underline{\sigma} = \sqrt{\nu} \nabla \mathbf{u} = \sqrt{\nu} (\nabla u_1, \nabla u_2)^\top$, then (1.1) can be rewritten as the following equivalent first-order differential system

$$(2.1) \quad \begin{cases} \frac{\partial \mathbf{u}}{\partial t} - \sqrt{\nu} \nabla \cdot \underline{\sigma} + \nabla \cdot (\boldsymbol{\gamma} \otimes \mathbf{u}) + \nabla p = \mathbf{f}, \\ \underline{\sigma} = \sqrt{\nu} \nabla \mathbf{u}, \\ \nabla \cdot \mathbf{u} = 0, \\ \mathbf{u}(\mathbf{x}, 0) = \mathbf{u}^0(\mathbf{x}). \end{cases}$$

Here the notations are the same as those in [7]. The gradient of the vector \mathbf{u} is a matrix, with $(\nabla \mathbf{u})_{ij} = \partial_j u_i$. The divergence of the matrix $\underline{\sigma}$ is a vector, with $(\nabla \cdot \underline{\sigma})_i = \sum_{j=1}^d \partial_j \sigma_{ij}$. $\boldsymbol{\gamma} \otimes \mathbf{u}$ is a matrix whose (i, j) th component is $\gamma_i u_j$.

We will define the semidiscrete LDG scheme based on equation (2.1). To this end, we would first like to give the finite element space and some notations.

2.1. Discontinuous finite element space. Let $\Omega_h = \{K\}$ be a quasi-uniform partition of the domain Ω with rectangular element K , where $h = \max_K h_K$, with h_K being the diameter of element K . We denote Γ_h as the set of all element interfaces. Associated with this mesh, we define the discontinuous finite element space

$$\begin{aligned} \Sigma_h &= \left\{ \underline{\sigma} \in L^2(\Omega)^{2 \times 2} : \underline{\sigma}|_K \in Q_k(K)^{2 \times 2} \quad \forall K \in \Omega_h \right\}, \\ \mathbf{V}_h &= \left\{ \mathbf{v} \in L^2(\Omega)^2 : \mathbf{v}|_K \in Q_k(K)^2 \quad \forall K \in \Omega_h \right\}, \\ Q_h &= \left\{ q \in L^2(\Omega) : q|_K \in Q_k(K) \quad \forall K \in \Omega_h, \text{ and } \int_{\Omega} q \, dx dy = 0 \right\}, \end{aligned}$$

which is contained in the following (mesh-dependent) broken Sobolev space $\underline{\Sigma} \times \mathbf{V} \times Q$:

$$\begin{aligned}\underline{\Sigma} &= \left\{ \underline{\sigma} \in L^2(\Omega)^{2 \times 2} : \underline{\sigma}|_K \in H^1(K)^{2 \times 2} \quad \forall K \in \Omega_h \right\}, \\ \mathbf{V} &= \left\{ \mathbf{v} \in L^2(\Omega)^2 : \mathbf{v}|_K \in H^1(K)^2 \quad \forall K \in \Omega_h \right\}, \\ Q &= \left\{ q \in L^2(\Omega) : q|_K \in H^1(K) \quad \forall K \in \Omega_h \text{ and } \int_{\Omega} q \, dx \, dy = 0 \right\},\end{aligned}$$

respectively. In this paper $\mathbf{Q}_k = \mathbf{P}_k \otimes \mathbf{P}_k$ denotes the space of the tensor product of polynomials of degree at most k .

2.2. Notations. We use a fixed vector $\beta = (1, 1)^\top$ to uniquely define the *left* and *right* elements K_L and K_R which share the same element interface e . Namely, $\beta \cdot \mathbf{n}_{K_L}|_e > 0$ and $\beta \cdot \mathbf{n}_{K_R}|_e < 0$, respectively, where \mathbf{n}_K is the outward normal of K . Along each side e , there are two traces for any function p , denoted by $p^+ = (p|_{K_R})|_e$ and $p^- = (p|_{K_L})|_e$, respectively, and we denote the *jump* by $[\![p]\!] = p^+ - p^-$ for scalar functions, $[\![\mathbf{v}]\!] = ([\![v_1]\!], [\![v_2]\!])^\top$ for vector-valued functions, and $[\![\underline{r}]\!] = ([\![r_{ij}]\!])_{2 \times 2}$ for matrix-valued functions. Besides, we use $\partial_K^- = \{e \subset \partial K, \beta \cdot \mathbf{n}_K|_e < 0\}$ and $\partial_K^+ = \{e \subset \partial K, \beta \cdot \mathbf{n}_K|_e > 0\}$ to denote the inflow and outflow sides of element K , respectively. For nonperiodic boundary conditions, we denote $\partial\Omega^- = \{e \subset \partial\Omega, \beta \cdot \mathbf{n}_e < 0\}$ and $\partial\Omega^+ = \{e \subset \partial\Omega, \beta \cdot \mathbf{n}_e > 0\}$ as the inflow and outflow boundaries, respectively.

In this paper, we will use the standard norms and semi-norms in the Sobolev space for scalar functions. For any given domain D , we denote by $\|w\|_D$ the L^2 norm of w on D . For any integer $s \geq 0$, let $H^s(D)$ represent the space equipped with the norm $\|\cdot\|_{s,D}$, in which the function itself and the derivatives up to the s th order are all in $L^2(D)$. If $D = \Omega$, we omit the subscript Ω for convenience. We define similar norms for vector-valued function \mathbf{u} and matrix-valued function $\underline{\sigma}$ as $\|\mathbf{u}\|_{s,D} = (\sum_{i=1}^d \|u_i\|_{s,D}^2)^{1/2}$ and $\|\underline{\sigma}\|_{s,D} = (\sum_{i,j=1}^d \|\sigma_{ij}\|_{s,D}^2)^{1/2}$, respectively. We also define $\|\mathbf{u}\|_{\Gamma_h} = (\sum_{e \in \Gamma_h} \|\mathbf{u}\|_e^2)^{1/2}$ and $\|\underline{\sigma}\|_{\Gamma_h} = (\sum_{e \in \Gamma_h} \|\underline{\sigma}\|_e^2)^{1/2}$. We denote $\|\nabla \mathbf{v}\| = (\sum_{K \in \Omega_h} \|\nabla \mathbf{v}\|_K^2)^{1/2}$ for $\mathbf{v} \in \mathbf{V}_h$.

In addition, we would like to write

$$\underline{\sigma} : \underline{r} = \sum_{i,j=1}^d \sigma_{ij} r_{ij}, \quad \mathbf{v} \cdot \underline{\sigma} \cdot \mathbf{n} = \sum_{i,j=1}^d v_i \sigma_{ij} n_j = \underline{\sigma} : (\mathbf{v} \otimes \mathbf{n}).$$

The symbol C is used as a generic constant, and ε is used to denote an arbitrary small constant, both C and ε may have different values in different occurrences. The symbol $\mu > 0$ is used to represent an inverse constant which appears in the following inverse inequalities:

$$(2.2) \quad \|\nabla \mathbf{v}\| \leq \mu h^{-1} \|\mathbf{v}\|, \quad \|\mathbf{v}\|_{\Gamma_h} \leq \sqrt{\mu h^{-1}} \|\mathbf{v}\|,$$

$$(2.3) \quad \|\underline{r}\|_{\Gamma_h} \leq \sqrt{\mu h^{-1}} \|\underline{r}\|$$

for any functions $\mathbf{v} \in \mathbf{V}_h$ and $\underline{r} \in \underline{\Sigma}_h$.

2.3. The semi-discrete LDG scheme. The LDG scheme for the Oseen equation (2.1) is to find the approximation $(\underline{\sigma}_h, \mathbf{u}_h, p_h) \in \underline{\Sigma}_h \times \mathbf{V}_h \times Q_h$, such that

the following variation forms hold for any element $K \in \Omega_h$ and any test function $(\underline{r}, \mathbf{v}, w) \in \underline{\Sigma}_h \times \mathbf{V}_h \times Q_h$,

$$(2.4a) \quad \int_K \frac{\partial \mathbf{u}_h}{\partial t} \cdot \mathbf{v} \, dx dy = \mathcal{H}_K(\mathbf{u}_h, \mathbf{v}) + \mathcal{L}_K(\underline{\sigma}_h, \mathbf{v}) + \mathcal{P}_K(p_h, \mathbf{v}),$$

$$(2.4b) \quad \int_K \underline{\sigma}_h : \underline{r} \, dx dy = \mathcal{K}_K(\mathbf{u}_h, \underline{r}),$$

$$(2.4c) \quad 0 = \mathcal{Q}_K(\mathbf{u}_h, w).$$

Here,

$$(2.5a) \quad \mathcal{H}_K(\mathbf{u}_h, \mathbf{v}) = \int_K (\boldsymbol{\gamma} \otimes \mathbf{u}_h) : \nabla \mathbf{v} \, dx dy - \int_{\partial K} \mathbf{v} \cdot \boldsymbol{\gamma} \otimes \widehat{\mathbf{u}_{h,\gamma}} \cdot \mathbf{n}_K \, ds,$$

$$(2.5b) \quad \mathcal{L}_K(\underline{\sigma}_h, \mathbf{v}) = -\sqrt{\nu} \left[\int_K \underline{\sigma}_h : \nabla \mathbf{v} \, dx dy - \int_{\partial K} \mathbf{v} \cdot \widehat{\underline{\sigma}_h} \cdot \mathbf{n}_K \, ds \right],$$

$$(2.5c) \quad \mathcal{P}_K(p_h, \mathbf{v}) = \int_K p_h \nabla \cdot \mathbf{v} \, dx dy - \int_{\partial K} \widehat{p_h} \mathbf{v} \cdot \mathbf{n}_K \, ds,$$

$$(2.5d) \quad \mathcal{K}_K(\mathbf{u}_h, \underline{r}) = -\sqrt{\nu} \left[\int_K \mathbf{u}_h \cdot \nabla \cdot \underline{r} \, dx dy - \int_{\partial K} \widehat{\mathbf{u}_{h,\sigma}} \cdot \underline{r} \cdot \mathbf{n}_K \, ds \right],$$

$$(2.5e) \quad \mathcal{Q}_K(\mathbf{u}_h, w) = \int_K \mathbf{u}_h \cdot \nabla w \, dx dy - \int_{\partial K} \widehat{\mathbf{u}_{h,p}} \cdot \mathbf{n}_K w \, ds.$$

The “hat” terms are the so-called numerical flux, which are taken as the “alternating” numerical flux

$$(2.6) \quad \begin{aligned} \widehat{\mathbf{u}_{h,\sigma}} &= \mathbf{u}_h^-, & \widehat{\underline{\sigma}_h} &= \underline{\sigma}_h^+, \\ \widehat{\mathbf{u}_{h,p}} &= \mathbf{u}_h^-, & \widehat{p_h} &= p_h^+ \end{aligned}$$

for the viscosity and the pressure terms. For the convection term, we can simply take the upwind numerical flux or the central flux. Since the convection velocity is assumed to be positive, we simply take the upwind flux

$$(2.7) \quad \widehat{\mathbf{u}_{h,\gamma}} = \mathbf{u}_h^-.$$

The initial condition $\mathbf{u}_h(\mathbf{x}, 0)$ can be taken as any approximation of the initial solution $\mathbf{u}^0(\mathbf{x})$, for example, the Stokes projection $\mathbf{\Pi}_h \mathbf{u}^0(\mathbf{x})$, which is to be defined in Section 3.

Denote $(\mathbf{u}, \mathbf{v}) = \sum_K \int_K \mathbf{u} \cdot \mathbf{v} \, dx dy$ and $(\sigma, r) = \sum_K \int_K \sigma : r \, dx dy$. Summing (2.4) over all elements K , we get the global form of the semi-discrete LDG scheme:

$$(2.8a) \quad (\mathbf{u}_{ht}, \mathbf{v}) = \mathcal{H}(\mathbf{u}_h, \mathbf{v}) + \mathcal{L}(\underline{\sigma}_h, \mathbf{v}) + \mathcal{P}(p_h, \mathbf{v}),$$

$$(2.8b) \quad (\underline{\sigma}_h, \underline{r}) = \mathcal{K}(\mathbf{u}_h, \underline{r}),$$

$$(2.8c) \quad 0 = \mathcal{Q}(\mathbf{u}_h, w).$$

Here $\Xi(\cdot, \cdot) = \sum_K \Xi_K(\cdot, \cdot)$ for $\Xi = \mathcal{H}, \mathcal{L}, \mathcal{P}, \mathcal{K}, \mathcal{Q}$. We have now defined the semi-discrete LDG scheme for the Oseen equation (2.1).

Remark 2.1. Integrating by parts gives rise to the following equivalent forms of (2.5):

$$(2.9a) \quad \mathcal{H}_K(\mathbf{u}_h, \mathbf{v}) = - \int_K (\mathbf{v} \otimes \boldsymbol{\gamma}) : \nabla \mathbf{u}_h \, dx dy + \int_{\partial_K^-} \mathbf{v} \cdot \boldsymbol{\gamma} \otimes [\![\mathbf{u}_h]\!] \cdot \mathbf{n}_K \, ds,$$

$$(2.9b) \quad \mathcal{L}_K(\underline{\sigma}_h, \mathbf{v}) = \sqrt{\nu} \left[\int_K \mathbf{v} \cdot (\nabla \cdot \underline{\sigma}_h) \, dx dy + \int_{\partial_K^+} \mathbf{v} \cdot [\![\underline{\sigma}_h]\!] \cdot \mathbf{n}_K \, ds \right],$$

$$(2.9c) \quad \mathcal{P}_K(p_h, \mathbf{v}) = - \int_K \mathbf{v} \cdot \nabla p_h \, dx dy - \int_{\partial_K^+} [p_h] \mathbf{v} \cdot \mathbf{n}_K \, ds,$$

$$(2.9d) \quad \mathcal{K}_K(\mathbf{u}_h, \underline{r}) = \sqrt{\nu} \left[\int_K \underline{r} : \nabla \mathbf{u}_h \, dx dy - \int_{\partial_K^-} [\![\mathbf{u}_h]\!] \cdot \underline{r} \cdot \mathbf{n}_K \, ds \right],$$

$$(2.9e) \quad \mathcal{Q}_K(\mathbf{u}_h, w) = - \int_K w \nabla \cdot \mathbf{u}_h \, dx dy + \int_{\partial_K^-} [\![\mathbf{u}_h]\!] \cdot \mathbf{n}_K w \, ds.$$

2.4. Properties of the LDG spatial discretization. In this subsection, we will give several lemmas to illustrate a few properties of the LDG spatial discretization. All the properties are trivial generalizations of the two-dimensional scalar case [18]. We refer the readers to [18] for the proof.

Lemma 2.1. *For any $\mathbf{u} \in \mathbf{V}$ and $\mathbf{v} \in \mathbf{V}_h$, there exists $C_\gamma = \|\boldsymbol{\gamma}\|$ independent of \mathbf{u} and \mathbf{v} such that*

$$(2.10) \quad \mathcal{H}(\mathbf{v}, \mathbf{v}) \leq 0,$$

$$(2.11) \quad |\mathcal{H}(\mathbf{u}, \mathbf{v})| \leq C_\gamma (\|\nabla \mathbf{u}\| + \sqrt{\mu h^{-1}} \|[\![\mathbf{u}]\!]\|_{\Gamma_h}) \|\mathbf{v}\|,$$

$$(2.12) \quad |\mathcal{H}(\mathbf{u}, \mathbf{v})| \leq C_\gamma \|\mathbf{u}\| (\|\nabla \mathbf{v}\| + \sqrt{\mu h^{-1}} \|[\![\mathbf{v}]\!]\|_{\Gamma_h}).$$

Lemma 2.2. *For any $p \in Q$ and $\mathbf{v} \in \mathbf{V}_h$, we have*

$$(2.13) \quad |\mathcal{P}(p, \mathbf{v})| \leq \|p\| (\|\nabla \mathbf{v}\| + \sqrt{\mu h^{-1}} \|[\![\mathbf{v}]\!]\|_{\Gamma_h}).$$

Lemma 2.3. *For any $(\underline{r}, \mathbf{v}, w) \in \underline{\Sigma}_h \times \mathbf{V}_h \times Q_h$, we have*

$$(2.14) \quad \mathcal{L}(\underline{r}, \mathbf{v}) + \mathcal{K}(\mathbf{v}, \underline{r}) = 0,$$

$$(2.15) \quad \mathcal{P}(w, \mathbf{v}) + \mathcal{Q}(\mathbf{v}, w) = 0.$$

The next lemma illustrates an important relationship between the gradient and the element interface jump of the numerical solution with the numerical solution of the gradient, which plays a key role in the stability and error analysis. Along a similar line as the proof in [18], we can obtain the proof of this lemma, hence it is omitted here.

Lemma 2.4. *Assume the pair of functions $(\mathbf{u}_h, \underline{\sigma}_h) \in \mathbf{V}_h \times \underline{\Sigma}_h$ satisfy (2.8b) for arbitrary $\underline{r} \in \underline{\Sigma}_h$, then*

$$(2.16) \quad \|\nabla \mathbf{u}_h\| + \sqrt{\mu h^{-1}} \|[\![\mathbf{u}_h]\!]\|_{\Gamma_h} \leq \frac{C_\mu}{\sqrt{\nu}} \|\underline{\sigma}_h\|,$$

where C_μ is a positive constant only depending on the inverse constant μ .

2.5. The inf-sup condition. We would like to begin this subsection by defining a projection \mathbf{P}_h following [5]: for any $\boldsymbol{\rho} \in H_0^1(\Omega)^2$, $\mathbf{P}_h \boldsymbol{\rho}|_K \in Q_k^2(K)$ satisfies

$$(2.17) \quad \begin{aligned} \int_K (\mathbf{P}_h \boldsymbol{\rho} - \boldsymbol{\rho}) \cdot \nabla v \, dx dy &= 0 \quad \forall v \in Q_k(K), \\ \int_e (\mathbf{P}_h \boldsymbol{\rho} - \boldsymbol{\rho}) \cdot \mathbf{n}_e v \, ds &= 0 \quad \forall v \in P_k(e), \forall e \in \partial_K^-. \end{aligned}$$

There holds the following approximation property [5]:

$$(2.18) \quad \|\boldsymbol{\rho} - \mathbf{P}_h \boldsymbol{\rho}\| + h|\boldsymbol{\rho} - \mathbf{P}_h \boldsymbol{\rho}|_1 + h^{1/2}\|\boldsymbol{\rho} - \mathbf{P}_h \boldsymbol{\rho}\|_{\Gamma_h} \leq Ch\|\boldsymbol{\rho}\|_1.$$

By (2.18) and the triangle inequality, we can easily get

$$(2.19) \quad \|\mathbf{P}_h \boldsymbol{\rho}\|_1 \leq C\|\boldsymbol{\rho}\|_1.$$

To get the estimate for the pressure, we will resort to the standard inf-sup argument in the analysis for Stokes problems. Since this argument will be used several times in this paper, we present the key results in the following lemma.

Lemma 2.5. *For arbitrary $q \in L_0^2(\Omega) \doteq \{v \in L^2(\Omega) | : \int_{\Omega} v = 0\}$, there exists $\mathbf{w}^* = \mathbf{w}^*(q) \in H_0^1(\Omega)^2$, such that*

$$(2.20) \quad - \int_{\Omega} q \nabla \cdot \mathbf{w}^* \, dx dy \geq \alpha_1 \|q\|^2, \quad \|\mathbf{w}^*\|_1 \leq \alpha_2 \|q\|,$$

for some positive constants α_1, α_2 independent of q , and

$$(2.21) \quad \|q\|^2 \leq C [\mathcal{K}(\mathbf{P}_h \mathbf{w}^*, \underline{r}) + \mathcal{Q}(\mathbf{P}_h \mathbf{w}^*, q) + \|\underline{r}\|^2]$$

for arbitrary $\underline{r} \in \underline{\Sigma}_h$, where \mathbf{P}_h is defined in (2.17).

Proof. The conclusion (2.20) is cited from [11]. Hence we only show (2.21).

On one hand, we have

$$(2.22) \quad \mathcal{Q}(\mathbf{P}_h \mathbf{w}^*, q) = \mathcal{Q}(\mathbf{w}^*, q) = - \int_{\Omega} q \nabla \cdot \mathbf{w}^* \, dx dy \geq \alpha_1 \|q\|^2$$

by the definition of \mathbf{P}_h and \mathcal{Q} , (2.9e) and (2.20), where we have used the fact that $\mathbf{w}^* \in H_0^1(\Omega)^2$ is continuous across the element interface.

On the other hand, for arbitrary $\underline{r} \in \underline{\Sigma}_h$, it follows from (2.9d) and the continuity of \mathbf{w}^* that

$$\mathcal{K}(\mathbf{w}^*, \underline{r}) = \sqrt{\nu} \int_{\Omega} \nabla \mathbf{w}^* : \underline{r} \, dx dy.$$

So

$$\begin{aligned} \mathcal{K}(\mathbf{P}_h \mathbf{w}^*, \underline{r}) &= \mathcal{K}(\mathbf{w}^*, \underline{r}) - \mathcal{K}(\mathbf{w}^* - \mathbf{P}_h \mathbf{w}^*, \underline{r}) = \sqrt{\nu} \int_{\Omega} \nabla \mathbf{w}^* : \underline{r} \, dx dy \\ &\quad - \sqrt{\nu} \sum_{K \in \Omega_h} \left[\int_K \nabla(\mathbf{w}^* - \mathbf{P}_h \mathbf{w}^*) : \underline{r} \, dx dy - \int_{\partial_K^-} [\mathbf{w}^* - \mathbf{P}_h \mathbf{w}^*] \cdot \underline{r} \cdot \mathbf{n}_K \, ds \right], \end{aligned}$$

where (2.9d) is used in the second line. Thus, by the aid of the Cauchy-Schwarz inequality and the trace inverse inequality (2.3), we get

$$|\mathcal{K}(\mathbf{P}_h \mathbf{w}^*, \underline{r})| \leq \sqrt{\nu} \|\mathbf{w}^*\|_1 \|\underline{r}\| + \sqrt{\nu} (|\mathbf{w}^* - \mathbf{P}_h \mathbf{w}^*|_1 + \sqrt{\mu h^{-1}} \|\mathbf{w}^* - \mathbf{P}_h \mathbf{w}^*\|_{\Gamma_h}) \|\underline{r}\|.$$

Then by the approximation property (2.18) we get

$$|\mathcal{K}(\mathbf{P}_h \mathbf{w}^*, \underline{r})| \leq C \|\mathbf{w}^*\|_1 \|\underline{r}\| \leq C \alpha_2 \|q\| \|\underline{r}\| \leq \frac{\alpha_1}{2} \|q\|^2 + \frac{C^2 \alpha_2^2}{2 \alpha_1} \|\underline{r}\|^2,$$

where we have used (2.20) and Young's inequality. So

$$(2.23) \quad \mathcal{K}(\mathbf{P}_h \mathbf{w}^*, \underline{r}) \geq -\frac{\alpha_1}{2} \|q\|^2 - \frac{C^2 \alpha_2^2}{2\alpha_1} \|\underline{r}\|^2.$$

Hence we obtain (2.21) immediately by adding up (2.22) and (2.23). This completes the proof of this lemma. \square

3. THE STOKES PROJECTION

In the later error analysis, the *Stokes projection* plays a salient role in obtaining the $L^\infty(L^2)$ optimal error estimates. The advantage of the Stokes projection lies in that the impact of pressure errors can be eliminated when estimating the velocity error. However, as far as we know, the Stokes projection associated with the LDG scheme has not been studied, and the approximation properties of the Stokes projection are not clear. Hence it is worth taking the effort to study it rigorously.

In this section, we will give the definition of the Stokes projection first, and then show the existence and uniqueness of the projection, the optimal approximation properties will be given and proven at the end of this section. To prove the optimal approximation properties, we need to resort to a series of projections which will be defined in Subsection 3.4. For the readers who are eager to enter into the stability and error analysis of the schemes, they can skip Subsections 3.4 and 3.5 for the time being.

3.1. The definition. Let $\mathbf{u} \in \mathbf{V}$ satisfy $\nabla \cdot \mathbf{u} = 0$, $\underline{\sigma} = \sqrt{\nu} \nabla \mathbf{u}$ and $p \in Q$, we define their Stokes projection $(\underline{\Pi}_h \underline{\sigma}, \mathbf{\Pi}_h \mathbf{u}, \Pi_h p) \in \underline{\Sigma}_h \times \mathbf{V}_h \times Q_h$ as follows: for arbitrary $(\underline{r}, \mathbf{v}, w) \in \underline{\Sigma}_h \times \mathbf{V}_h \times Q_h$, it holds that

$$(3.1a) \quad \mathcal{L}(\underline{\Pi}_h \underline{\sigma}, \mathbf{v}) + \mathcal{P}(\Pi_h p, \mathbf{v}) = \mathcal{L}(\underline{\sigma}, \mathbf{v}) + \mathcal{P}(p, \mathbf{v}),$$

$$(3.1b) \quad (\underline{\Pi}_h \underline{\sigma}, \underline{r}) = \mathcal{K}(\mathbf{\Pi}_h \mathbf{u}, \underline{r}),$$

$$(3.1c) \quad \mathcal{Q}(\mathbf{\Pi}_h \mathbf{u}, w) = \mathcal{Q}(\mathbf{u}, w).$$

In addition, to ensure the uniqueness of the projection, we let

$$(3.1d) \quad \int_{\Omega} (\mathbf{\Pi}_h \mathbf{u} - \mathbf{u}) \cdot \mathbf{e}_i \, dx dy = 0 \quad \text{for } i = 1, 2,$$

where $\mathbf{e}_1 = (1, 0)^\top$ and $\mathbf{e}_2 = (0, 1)^\top$, and

$$(3.1e) \quad \int_{\Omega} (\Pi_h p - p) \, dx dy = 0.$$

Remark 3.1. The condition (3.1e) holds automatically since the averages of both p and $\Pi_h p$ are 0.

3.2. Existence and uniqueness.

Lemma 3.1. *The projection defined in (3.1) exists uniquely.*

Proof. To show that the Stokes projection exists uniquely, it is enough to show that, if $(\underline{\sigma}, \mathbf{u}, p) = (\underline{0}, \mathbf{0}, 0)$, then the only possible solution of $(\underline{\Pi}_h \underline{\sigma}, \mathbf{\Pi}_h \mathbf{u}, \Pi_h p)$ defined in (3.1) equals $(\underline{0}, \mathbf{0}, 0)$. To this end, we consider

$$(3.2a) \quad 0 = \mathcal{L}(\underline{\Pi}_h \underline{\sigma}, \mathbf{v}) + \mathcal{P}(\Pi_h p, \mathbf{v}),$$

$$(3.2b) \quad (\underline{\Pi}_h \underline{\sigma}, \underline{r}) = \mathcal{K}(\mathbf{\Pi}_h \mathbf{u}, \underline{r}),$$

$$(3.2c) \quad 0 = \mathcal{Q}(\mathbf{\Pi}_h \mathbf{u}, w).$$

Taking $(\underline{r}, \mathbf{v}, w) = (\underline{\Pi_h \sigma}, \mathbf{\Pi}_h \mathbf{u}, \Pi_h p)$ in (3.2) and adding them together leads to $\|\underline{\Pi_h \sigma}\|^2 = 0$ by Lemma 2.3. Hence $\underline{\Pi_h \sigma} = \underline{0}$, thus it follows from (3.2b) that (3.3)

$$0 = \mathcal{K}(\mathbf{\Pi}_h \mathbf{u}, \underline{r}) = -\sqrt{\nu} \sum_{K \in \Omega_h} \left[\int_K \mathbf{\Pi}_h \mathbf{u} \cdot \nabla \cdot \underline{r} \, dx dy - \int_{\partial_K} (\mathbf{\Pi}_h \mathbf{u})^- \cdot \underline{r} \cdot \mathbf{n}_K \, ds \right].$$

By taking $\underline{r} = \mathbf{\Pi}_h \mathbf{u} \otimes \boldsymbol{\beta}$, where $\boldsymbol{\beta} = (1, 1)^\top$, we get

$$(3.4) \quad \sum_{K \in \Omega_h} \left[\int_K \mathbf{\Pi}_h \mathbf{u} \cdot \nabla \cdot (\mathbf{\Pi}_h \mathbf{u} \otimes \boldsymbol{\beta}) \, dx dy - \int_{\partial_K} (\mathbf{\Pi}_h \mathbf{u} \otimes \boldsymbol{\beta}) : ((\mathbf{\Pi}_h \mathbf{u})^- \otimes \mathbf{n}_K) \, ds \right] = 0.$$

Noting that

$$\int_K \mathbf{\Pi}_h \mathbf{u} \cdot \nabla \cdot (\mathbf{\Pi}_h \mathbf{u} \otimes \boldsymbol{\beta}) \, dx dy = \frac{1}{2} \int_{\partial_K} (\mathbf{\Pi}_h \mathbf{u} \otimes \boldsymbol{\beta}) : (\mathbf{\Pi}_h \mathbf{u} \otimes \mathbf{n}_K) \, ds.$$

Thus (3.4) becomes

$$\begin{aligned} & \sum_{K \in \Omega_h} \left[\frac{1}{2} \int_{\partial_K^-} ((\mathbf{\Pi}_h \mathbf{u})^+ \otimes \boldsymbol{\beta}) : ((\mathbf{\Pi}_h \mathbf{u})^+ \otimes \mathbf{n}_K) \, ds \right. \\ & \quad - \frac{1}{2} \int_{\partial_K^+} ((\mathbf{\Pi}_h \mathbf{u})^- \otimes \boldsymbol{\beta}) : ((\mathbf{\Pi}_h \mathbf{u})^- \otimes \mathbf{n}_K) \, ds \\ & \quad \left. - \int_{\partial_K^-} ((\mathbf{\Pi}_h \mathbf{u})^+ \otimes \boldsymbol{\beta}) : ((\mathbf{\Pi}_h \mathbf{u})^- \otimes \mathbf{n}_K) \, ds \right] = 0, \end{aligned}$$

which is equivalent to

$$\begin{aligned} & \sum_{e \in \Gamma_h} \frac{1}{2} \int_e [(\mathbf{\Pi}_h \mathbf{u})^+ \cdot (\mathbf{\Pi}_h \mathbf{u})^+ - 2(\mathbf{\Pi}_h \mathbf{u})^+ \cdot (\mathbf{\Pi}_h \mathbf{u})^- + (\mathbf{\Pi}_h \mathbf{u})^- \cdot (\mathbf{\Pi}_h \mathbf{u})^-] (\boldsymbol{\beta} \cdot \mathbf{n}_e) \, ds \\ &= \sum_{e \in \Gamma_h} \frac{1}{2} \int_e [\llbracket \mathbf{\Pi}_h \mathbf{u} \rrbracket \cdot \llbracket \mathbf{\Pi}_h \mathbf{u} \rrbracket] (\boldsymbol{\beta} \cdot \mathbf{n}_e) = 0, \end{aligned}$$

by the periodic boundary condition, here $\boldsymbol{\beta} \cdot \mathbf{n}_e < 0$ for all $e \in \Gamma_h$. It implies $\mathbf{\Pi}_h \mathbf{u}$ is continuous across each element interface. Hence, from (3.3) and integrating by parts, we have

$$(3.5) \quad \sum_{K \in \Omega_h} \left[\int_K \nabla \mathbf{\Pi}_h \mathbf{u} : \underline{r} \, dx dy - \int_{\partial_K} \llbracket \mathbf{\Pi}_h \mathbf{u} \rrbracket \cdot \underline{r} \cdot \mathbf{n}_K \, ds \right] = \sum_{K \in \Omega_h} \int_K \nabla \mathbf{\Pi}_h \mathbf{u} : \underline{r} \, dx dy = 0.$$

Choosing $\underline{r} = \nabla \mathbf{\Pi}_h \mathbf{u}$, we get $\nabla \mathbf{\Pi}_h \mathbf{u} = \underline{0}$ in each element K , which implies that $\mathbf{\Pi}_h \mathbf{u}$ is a constant. Then according to the condition (3.1d) we deduce that $\mathbf{\Pi}_h \mathbf{u} = \mathbf{0}$.

Along a similar line as above, we can obtain $\Pi_h p = 0$. Thus we have completed the proof of this lemma. \square

3.3. The approximation property. To obtain the optimal approximation properties of the Stokes projection (3.1), we will resort to the following adjoint Stokes

problem similar as that considered in [3, 7],

$$(3.6a) \quad -\sqrt{\nu} \nabla \cdot \underline{s} + \nabla q = \boldsymbol{\lambda}, \quad \text{in } \Omega,$$

$$(3.6b) \quad \underline{s} = \sqrt{\nu} \nabla \mathbf{z}, \quad \text{in } \Omega,$$

$$(3.6c) \quad \nabla \cdot \mathbf{z} = 0, \quad \text{in } \Omega$$

for any given $\boldsymbol{\lambda} \in L^2(\Omega)^2$, with the periodic boundary condition and $\int_{\Omega} q = 0$. In addition, we assume it satisfies the following elliptic regularity assumption

$$(3.7) \quad \nu \|\mathbf{z}\|_2 + \sqrt{\nu} \|\underline{s}\|_1 + \|q\|_1 \leq C_* \|\boldsymbol{\lambda}\|.$$

The approximation property of the Stokes projection is stated as follows.

Lemma 3.2. *Assume $\mathbf{u} \in H^{k+2}(\Omega)^2$, $\underline{\sigma} = \sqrt{\nu} \nabla \mathbf{u} \in H^{k+1}(\Omega)^{2 \times 2}$ and $p \in H^{k+2}(\Omega)$ satisfies $\int_{\Omega} p = 0$, then there exists a bounding constant C depending on the regularity of $(\mathbf{u}, \underline{\sigma}, p)$ and the elliptic regularity constant C_* defined in (3.7), such that*

$$(3.8) \quad \|\mathbf{u} - \mathbf{\Pi}_h \mathbf{u}\| + \|\underline{\sigma} - \underline{\Pi}_h \underline{\sigma}\| + \|p - \Pi_h p\| \leq Ch^{k+1}.$$

We will prove this lemma in Subsection 3.5.

3.4. Useful projections. To prove Lemma 3.2, we would like to introduce another series of projections $(\underline{\pi}_h, \boldsymbol{\pi}_h, \pi_h) : \underline{\Sigma} \times \mathbf{V} \times Q \rightarrow \underline{\Sigma}_h \times \mathbf{V}_h \times Q_h$, corresponding to matrix-valued functions, vector-valued functions and scalar functions, respectively. To define these projections conveniently, we would like to represent any rectangular element as $K = I_i \times J_j$, where $I_i = (x_{i-\frac{1}{2}}, x_{i+\frac{1}{2}})$ and $J_j = (y_{j-\frac{1}{2}}, y_{j+\frac{1}{2}})$. In what follows, we will present these useful projections and their properties.

First we define two projections π_h^+ and π_h^- from $H^1(\Omega_h) = \{v \in L^2(\Omega) : v|_K \in H^1(K) \forall K \in \Omega_h\}$ onto $W_h = \{v \in L^2(\Omega) : v|_K \in Q_k(K) \forall K \in \Omega_h\}$, following [15]:

$$\begin{aligned} & \int_K (\pi_h^+ w - w)v \, dx \, dy = 0 \quad \forall v \in Q_{k-1}(K), \\ & \int_{J_j} (\pi_h^+ w - w)_{i-\frac{1}{2}, y} v \, dy = 0 \quad \forall v \in P_{k-1}(J_j), \\ & \int_{I_i} (\pi_h^+ w - w)_{x, j-\frac{1}{2}} v \, dx = 0 \quad \forall v \in P_{k-1}(I_i), \\ & \pi_h^+ w(x_{i-\frac{1}{2}}, y_{j-\frac{1}{2}}) = w(x_{i-\frac{1}{2}}, y_{j-\frac{1}{2}}) \quad \forall i \forall j, \end{aligned}$$

and

$$\begin{aligned} & \int_K (\pi_h^- w - w)v \, dx \, dy = 0 \quad \forall v \in Q_{k-1}(K), \\ & \int_{J_j} (\pi_h^- w - w)_{i+\frac{1}{2}, y} v \, dy = 0 \quad \forall v \in P_{k-1}(J_j), \\ & \int_{I_i} (\pi_h^- w - w)_{x, j+\frac{1}{2}} v \, dx = 0 \quad \forall v \in P_{k-1}(I_i), \\ & \pi_h^- w(x_{i+\frac{1}{2}}, y_{j+\frac{1}{2}}) = w(x_{i+\frac{1}{2}}, y_{j+\frac{1}{2}}) \quad \forall i \forall j. \end{aligned}$$

Next we are going to define the projections $(\underline{\pi}_h, \boldsymbol{\pi}_h, \pi_h)$, based on the projections defined above and the projection \mathbf{P}_h defined in (2.17).

- (1) For matrix-valued function $\underline{\sigma} = (\sigma_1, \sigma_2) \in \Sigma$, where σ_1 and σ_2 are its two column vectors, we define

$$(3.9) \quad \underline{\pi}_h \underline{\sigma} = (\mathbf{P}_h \sigma_1, \mathbf{P}_h \sigma_2).$$

- (2) For vector-valued function $\mathbf{u} = (u_1, u_2)^\top \in \mathbf{V}$, we define

$$(3.10) \quad \boldsymbol{\pi}_h \mathbf{u} = (\pi_h^- u_1, \pi_h^- u_2)^\top.$$

- (3) For scalar function $p \in Q$, we define

$$(3.11) \quad \pi_h p = \pi_h^+ p.$$

The following properties of these projections hold:

- (1) For arbitrary $\mathbf{v} \in \mathbf{V}_h$, we have

$$(3.12) \quad \mathcal{L}(\underline{\sigma} - \underline{\pi}_h \underline{\sigma}, \mathbf{v}) = 0.$$

- (2) For arbitrary $\underline{\sigma} \in H^s(\Omega)^{2 \times 2}$, $\mathbf{u} \in H^s(\Omega)^2$ and $p \in H^s(\Omega)$ with $s \geq 1$, by the standard scaling argument [4], along a similar analysis as in [5], we can obtain the following approximation properties:

$$(3.13a) \quad \|\underline{\sigma} - \underline{\pi}_h \underline{\sigma}\| + h|\underline{\sigma} - \underline{\pi}_h \underline{\sigma}|_1 + h^{1/2}\|\underline{\sigma} - \underline{\pi}_h \underline{\sigma}\|_{\Gamma_h} \leq Ch^{\min\{k+1,s\}}\|\underline{\sigma}\|_s,$$

$$(3.13b) \quad \|\mathbf{u} - \boldsymbol{\pi}_h \mathbf{u}\| + h|\mathbf{u} - \boldsymbol{\pi}_h \mathbf{u}|_1 + h^{1/2}\|\mathbf{u} - \boldsymbol{\pi}_h \mathbf{u}\|_{\Gamma_h} \leq Ch^{\min\{k+1,s\}}\|\mathbf{u}\|_s,$$

$$(3.13c) \quad \|p - \pi_h p\| + h|p - \pi_h p|_1 + h^{1/2}\|p - \pi_h p\|_{\Gamma_h} \leq Ch^{\min\{k+1,s\}}\|p\|_s.$$

- (3) From [5], we can also get the following superconvergence properties: suppose $\mathbf{u} \in H^{k+2}(\Omega)^2$ and $p \in H^{k+2}(\Omega)$, then

$$(3.14a) \quad |\mathcal{P}(p - \pi_h p, \mathbf{v})| \leq Ch^{k+1}\|p\|_{k+2}\|\mathbf{v}\|,$$

$$(3.14b) \quad |\mathcal{K}(\mathbf{u} - \boldsymbol{\pi}_h \mathbf{u}, \underline{r})| \leq C\sqrt{\nu}h^{k+1}\|\mathbf{u}\|_{k+2}\|\underline{r}\|,$$

$$(3.14c) \quad |\mathcal{Q}(\mathbf{u} - \boldsymbol{\pi}_h \mathbf{u}, w)| \leq Ch^{k+1}\|\mathbf{u}\|_{k+2}\|w\|.$$

3.5. Proof of Lemma 3.2. For the simplicity of notation, we denote by $\boldsymbol{\eta} = (\underline{\eta}_{\sigma}, \boldsymbol{\eta}_{\mathbf{u}}, \eta_p) = (\Pi_h \underline{\sigma} - \underline{\sigma}, \Pi_h \mathbf{u} - \mathbf{u}, \Pi_h p - p)$. We begin the proof with the following relationship:

$$(3.15a) \quad 0 = \mathcal{L}(\underline{\eta}_{\sigma}, \mathbf{v}) + \mathcal{P}(\eta_p, \mathbf{v}),$$

$$(3.15b) \quad (\underline{\eta}_{\sigma}, \underline{r}) = \mathcal{K}(\boldsymbol{\eta}_{\mathbf{u}}, \underline{r}),$$

$$(3.15c) \quad 0 = \mathcal{Q}(\boldsymbol{\eta}_{\mathbf{u}}, w),$$

for any test function $(\underline{r}, \mathbf{v}, w) \in \Sigma_h \times \mathbf{V}_h \times Q_h$.

Based on the projections defined in Subsection 3.4, we split the error $\boldsymbol{\eta} = (\underline{\eta}_{\sigma}, \boldsymbol{\eta}_{\mathbf{u}}, \eta_p)$ into two parts, namely

$$(3.16) \quad \underline{\eta}_{\sigma} = \underline{\sigma} - \underline{\pi}_h \underline{\sigma} + \underline{\pi}_h \underline{\eta}_{\sigma}, \quad \boldsymbol{\eta}_{\mathbf{u}} = \mathbf{u} - \boldsymbol{\pi}_h \mathbf{u} + \boldsymbol{\pi}_h \boldsymbol{\eta}_{\mathbf{u}}, \quad \eta_p = p - \pi_h p + \pi_h \eta_p.$$

Thus, to prove Lemma 3.2, the remaining work is to estimate $(\underline{\pi}_h \underline{\eta}_{\sigma}, \boldsymbol{\pi}_h \boldsymbol{\eta}_{\mathbf{u}}, \pi_h \eta_p)$ in a sharp way, since (3.13) hold. To do that, we will proceed in three steps.

Step 1. First we give the estimate for $\|\underline{\pi}_h \underline{\eta}_{\sigma}\|$. By (3.15) and the division of $\boldsymbol{\eta}$ (3.16), we have

$$(3.17a) \quad -\mathcal{L}(\underline{\pi}_h \underline{\eta}_{\sigma}, \mathbf{v}) - \mathcal{P}(\pi_h \eta_p, \mathbf{v}) = \mathcal{L}(\underline{\sigma} - \underline{\pi}_h \underline{\sigma}, \mathbf{v}) + \mathcal{P}(p - \pi_h p, \mathbf{v}),$$

$$(3.17b) \quad (\underline{\pi}_h \underline{\eta}_{\sigma}, \underline{r}) - \mathcal{K}(\boldsymbol{\pi}_h \boldsymbol{\eta}_{\mathbf{u}}, \underline{r}) = -(\underline{\sigma} - \underline{\pi}_h \underline{\sigma}, \underline{r}) + \mathcal{K}(\mathbf{u} - \boldsymbol{\pi}_h \mathbf{u}, \underline{r}),$$

$$(3.17c) \quad -\mathcal{Q}(\boldsymbol{\pi}_h \boldsymbol{\eta}_{\mathbf{u}}, w) = \mathcal{Q}(\mathbf{u} - \boldsymbol{\pi}_h \mathbf{u}, w).$$

Noting the error's orthogonal property (3.12), taking $(\underline{r}, \mathbf{v}, w) = (\underline{\pi_h \eta_\sigma}, \boldsymbol{\pi_h \eta_u}, \pi_h \eta_p)$ in (3.17), and adding the three equalities together, we obtain

$$\begin{aligned} \|\underline{\pi_h \eta_\sigma}\|^2 &= -(\underline{\sigma} - \underline{\pi_h \sigma}, \underline{\pi_h \eta_\sigma}) + \mathcal{P}(p - \pi_h p, \boldsymbol{\pi_h \eta_u}) + \mathcal{K}(\mathbf{u} - \boldsymbol{\pi_h u}, \underline{\pi_h \eta_\sigma}) \\ &\quad + \mathcal{Q}(\mathbf{u} - \boldsymbol{\pi_h u}, \pi_h \eta_p), \end{aligned}$$

where the left-hand side is owing to Lemma 2.3. By applying the Cauchy-Schwarz inequality and the approximation property (3.13a) to the first term on the right-hand side, and the superconvergence properties (3.14) to the remaining three terms, we obtain

$$\begin{aligned} \|\underline{\pi_h \eta_\sigma}\|^2 &\leq Ch^{k+1}(\|\underline{\pi_h \eta_\sigma}\| + \|\boldsymbol{\pi_h \eta_u}\| + \|\pi_h \eta_p\|) \\ (3.18) \quad &\leq \varepsilon(\|\underline{\pi_h \eta_\sigma}\|^2 + \|\boldsymbol{\pi_h \eta_u}\|^2 + \|\pi_h \eta_p\|^2) + Ch^{2k+2} \end{aligned}$$

for arbitrary $\varepsilon > 0$, where Young's inequality is used in the last inequality. Thus by choosing ε small enough, we get

$$(3.19) \quad \|\underline{\pi_h \eta_\sigma}\|^2 \leq Ch^{2k+2} + \varepsilon(\|\boldsymbol{\pi_h \eta_u}\|^2 + \|\pi_h \eta_p\|^2).$$

Step 2. We would like to estimate $\|\pi_h \eta_p\|$ in this step. Owing to Lemma 2.5, for $\pi_h \eta_p \in L_0^2(\Omega)$, there exists $\mathbf{v}^* \in H_0^1(\Omega)^2$ such that $\|\mathbf{v}^*\|_1 \leq \alpha_2 \|\pi_h \eta_p\|$ and

$$(3.20) \quad \|\pi_h \eta_p\|^2 \leq C \underbrace{[\mathcal{K}(\mathbf{P}_h \mathbf{v}^*, \underline{\pi_h \eta_\sigma}) + \mathcal{Q}(\mathbf{P}_h \mathbf{v}^*, \pi_h \eta_p) + \|\underline{\pi_h \eta_\sigma}\|^2]}_Z,$$

where we choose $\underline{r} = \underline{\pi_h \eta_\sigma}$ in (2.21). By using Lemma 2.3, (3.17a) and the error's orthogonal property (3.12) successively, we get

$$(3.21) \quad Z = -\mathcal{L}(\underline{\pi_h \eta_\sigma}, \mathbf{P}_h \mathbf{v}^*) - \mathcal{P}(\pi_h \eta_p, \mathbf{P}_h \mathbf{v}^*) = \mathcal{P}(p - \pi_h p, \mathbf{P}_h \mathbf{v}^*).$$

Thus, by using the superconvergence property (3.14a), (2.19), (2.20), and the Young's inequality, we have

$$(3.22) \quad Z \leq Ch^{k+1} \|\mathbf{P}_h \mathbf{v}^*\| \leq Ch^{k+1} \|\mathbf{v}^*\|_1 \leq C \alpha_2 h^{k+1} \|\pi_h \eta_p\| \leq \varepsilon \|\pi_h \eta_p\|^2 + Ch^{2k+2}.$$

Consequently, we get

$$(3.23) \quad \|\pi_h \eta_p\|^2 \leq Ch^{2k+2} + C \|\underline{\pi_h \eta_\sigma}\|^2 \leq Ch^{2k+2} + \varepsilon(\|\boldsymbol{\pi_h \eta_u}\|^2 + \|\pi_h \eta_p\|^2),$$

by using the estimate (3.19). Hence choosing ε small enough gives rise to

$$(3.24) \quad \|\pi_h \eta_p\|^2 \leq Ch^{2k+2} + \varepsilon \|\boldsymbol{\pi_h \eta_u}\|^2.$$

Step 3. In this step we will estimate $\|\boldsymbol{\pi_h \eta_u}\|$. For arbitrary $\boldsymbol{\lambda} \in L^2(\Omega)^2$, let $\mathbf{z}, \underline{s}, q$ be defined in the adjoint Stokes problem (3.6), then from (3.6) we have

$$\begin{aligned} (3.25) \quad &(\boldsymbol{\pi_h \eta_u}, \boldsymbol{\lambda}) \\ &= (\boldsymbol{\pi_h \eta_u}, -\sqrt{\nu} \nabla \cdot \underline{s} + \nabla q) = -\mathcal{L}(\underline{s}, \boldsymbol{\pi_h \eta_u}) - \mathcal{P}(q, \boldsymbol{\pi_h \eta_u}) \\ &= \mathcal{L}(\underline{\pi_h s} - \underline{s}, \boldsymbol{\pi_h \eta_u}) - \mathcal{L}(\underline{\pi_h s}, \boldsymbol{\pi_h \eta_u}) + \mathcal{P}(\pi_h q - q, \boldsymbol{\pi_h \eta_u}) - \mathcal{P}(\pi_h q, \boldsymbol{\pi_h \eta_u}) \\ &= \mathcal{K}(\boldsymbol{\pi_h \eta_u}, \underline{\pi_h s}) + \mathcal{P}(\pi_h q - q, \boldsymbol{\pi_h \eta_u}) + \mathcal{Q}(\boldsymbol{\pi_h \eta_u}, \pi_h q) \\ &= (\underline{\eta_\sigma}, \underline{\pi_h s}) + \mathcal{K}(\boldsymbol{\pi_h u} - \mathbf{u}, \underline{\pi_h s}) + \mathcal{P}(\pi_h q - q, \boldsymbol{\pi_h \eta_u}) + \mathcal{Q}(\boldsymbol{\pi_h u} - \mathbf{u}, \pi_h q) \\ &= V_1 + V_2 + V_3 + V_4, \end{aligned}$$

where we have used (2.9b), (2.9c), and the continuity of \underline{s} and q in the first line, the error's orthogonal property (3.12) and Lemma 2.3 in the third line, and the properties (3.17b), (3.17c) in the fourth line.

Next we turn to estimate each term on the right-hand side of (3.25). First, by using the Cauchy-Schwarz inequality, the triangle inequality, the approximation property (3.13a) and the elliptic regularity (3.7) we get

$$(3.26) \quad |V_1| \leq \|\underline{\eta}_\sigma\| \|\pi_h \underline{s}\| \leq C(\|\underline{\sigma} - \underline{\pi}_h \underline{\sigma}\| + \|\pi_h \underline{\eta}_\sigma\|) \|\underline{s}\|_1 \leq \frac{CC_*}{\sqrt{\nu}} (h^{k+1} + \|\pi_h \underline{\eta}_\sigma\|) \|\lambda\|.$$

Second, due to the superconvergence property (3.14) we have

$$(3.27) \quad |V_2 + V_4| \leq Ch^{k+1} (\sqrt{\nu} \|\pi_h \underline{s}\| + \|\pi_h q\|) \leq Ch^{k+1} (\sqrt{\nu} \|\underline{s}\|_1 + \|q\|_1) \leq CC_* h^{k+1} \|\lambda\|.$$

Third, from (3.17b) we can derive that

$$(3.28) \quad \|\nabla \pi_h \boldsymbol{\eta}_u\| + \sqrt{\mu h^{-1}} \|\llbracket \pi_h \boldsymbol{\eta}_u \rrbracket\|_{\Gamma_h} \leq \frac{C_\mu}{\sqrt{\nu}} (h^{k+1} + \|\pi_h \underline{\eta}_\sigma\|).$$

The proof of this relationship is similar to but a little more complicated than the proof for Lemma 2.4, so we only give the idea of the proof and omit the details to save space. According to (3.17b), we choose suitable test functions \underline{r} (refer to [18]), then we can get (3.28) by using the Cauchy-Schwarz inequality for the terms $(\pi_h \underline{\eta}_\sigma, \underline{r})$ and $(\underline{\sigma} - \underline{\pi}_h \underline{\sigma}, \underline{r})$, and the superconvergence property (3.14b) for the term $\mathcal{K}(\boldsymbol{u} - \boldsymbol{\Pi}_h \boldsymbol{u}, \underline{r})$.

Hence, a simple application of Lemma 2.2, the approximation property (3.13c), (3.28) and the elliptic regularity (3.7) yields

$$(3.29) \quad \begin{aligned} |V_3| &\leq C \|\pi_h q - q\| (\|\nabla \pi_h \boldsymbol{\eta}_u\| + \sqrt{\mu h^{-1}} \|\llbracket \pi_h \boldsymbol{\eta}_u \rrbracket\|_{\Gamma_h}) \\ &\leq \frac{CC_\mu}{\sqrt{\nu}} h \|q\|_1 (h^{k+1} + \|\pi_h \underline{\eta}_\sigma\|) \leq \frac{CC_* C_\mu}{\sqrt{\nu}} h (h^{k+1} + \|\pi_h \underline{\eta}_\sigma\|) \|\lambda\|. \end{aligned}$$

As a consequence, by taking $\lambda = \pi_h \boldsymbol{\eta}_u$, we can derive

$$(3.30) \quad \|\pi_h \boldsymbol{\eta}_u\| \leq C(h/\sqrt{\nu} + 1/\sqrt{\nu} + 1)(h^{k+1} + \|\pi_h \underline{\eta}_\sigma\|) \leq Ch^{k+1} + \varepsilon \|\pi_h \boldsymbol{\eta}_u\|,$$

where ε is an arbitrary small value. Thus, if we take ε small enough we can get

$$(3.31) \quad \|\pi_h \boldsymbol{\eta}_u\| \leq Ch^{k+1}.$$

As a result, we get

$$(3.32) \quad \|\pi_h \eta_p\| \leq Ch^{k+1} \quad \text{and} \quad \|\pi_h \underline{\eta}_\sigma\| \leq Ch^{k+1}$$

from (3.24) and (3.19). Consequently, (3.8) follows by the triangle inequality, this completes the proof of Lemma 3.2. \square

4. THE FULLY-DISCRETE SCHEMES AND THEIR STABILITY ANALYSIS

4.1. The fully-discrete schemes. In this subsection we would like to present the fully-discrete LDG schemes coupled with three specific multi-step IMEX time-marching methods up to the third order, which have been considered in [17] for one-dimensional convection-diffusion equations.

Let $\{t^n = n\tau\}_{n=0}^M$ be the uniform partition of the time interval $[0, T]$, with time-step τ such that $M\tau = T$. Given \boldsymbol{u}_h^n , we would like to find the numerical solution

(\mathbf{u}_h, p_h) at the next time level t^{n+1} by the multi-step IMEX time-marching schemes which were developed in [12].

First order:

$$(4.1a) \quad (\mathbf{u}_h^{n+1}, \mathbf{v}) = (\mathbf{u}_h^n, \mathbf{v}) + \tau[\mathcal{H}(\mathbf{u}_h^n, \mathbf{v}) + \mathcal{L}(\underline{\sigma}_h^{n+1}, \mathbf{v}) + \mathcal{P}(p_h^{n+1}, \mathbf{v})],$$

$$(4.1b) \quad (\underline{\sigma}_h^{n+1}, \underline{r}) = \mathcal{K}(\mathbf{u}_h^{n+1}, \underline{r}),$$

$$(4.1c) \quad 0 = \mathcal{Q}(\mathbf{u}_h^{n+1}, w) \quad \forall n \geq 0.$$

Second order:

$$\begin{aligned} (4.2a) \quad & (\mathbf{u}_h^{n+1}, \mathbf{v}) = (\mathbf{u}_h^n, \mathbf{v}) + \frac{3}{2}\tau\mathcal{H}(\mathbf{u}_h^n, \mathbf{v}) - \frac{1}{2}\tau\mathcal{H}(\mathbf{u}_h^{n-1}, \mathbf{v}) \\ & + \frac{3}{4}\tau\mathcal{L}(\underline{\sigma}_h^{n+1}, \mathbf{v}) + \frac{1}{4}\tau\mathcal{L}(\underline{\sigma}_h^{n-1}, \mathbf{v}) \\ & + \frac{3}{4}\tau\mathcal{P}(p_h^{n+1}, \mathbf{v}) + \frac{1}{4}\tau\mathcal{P}(p_h^{n-1}, \mathbf{v}) \quad \forall n \geq 1, \end{aligned}$$

$$(4.2b) \quad (\underline{\sigma}_h^n, \underline{r}) = \mathcal{K}(\mathbf{u}_h^n, \underline{r}) \quad \forall n \geq 0,$$

$$(4.2c) \quad 0 = \mathcal{Q}(\mathbf{u}_h^n, w) \quad \forall n \geq 0.$$

Third order:

$$\begin{aligned} (4.3a) \quad & (\mathbf{u}_h^{n+1}, \mathbf{v}) = (\mathbf{u}_h^n, \mathbf{v}) + \frac{23}{12}\tau\mathcal{H}(\mathbf{u}_h^n, \mathbf{v}) - \frac{4}{3}\tau\mathcal{H}(\mathbf{u}_h^{n-1}, \mathbf{v}) + \frac{5}{12}\tau\mathcal{H}(\mathbf{u}_h^{n-2}, \mathbf{v}) \\ & + \frac{2}{3}\tau\mathcal{L}(\underline{\sigma}_h^{n+1}, \mathbf{v}) + \frac{5}{12}\tau\mathcal{L}(\underline{\sigma}_h^{n-1}, \mathbf{v}) - \frac{1}{12}\tau\mathcal{L}(\underline{\sigma}_h^{n-3}, \mathbf{v}) \\ & + \frac{2}{3}\tau\mathcal{P}(p_h^{n+1}, \mathbf{v}) + \frac{5}{12}\tau\mathcal{P}(p_h^{n-1}, \mathbf{v}) - \frac{1}{12}\tau\mathcal{P}(p_h^{n-3}, \mathbf{v}) \quad \forall n \geq 3, \end{aligned}$$

$$(4.3b) \quad (\underline{\sigma}_h^n, \underline{r}) = \mathcal{K}(\mathbf{u}_h^n, \underline{r}) \quad \forall n \geq 0,$$

$$(4.3c) \quad 0 = \mathcal{Q}(\mathbf{u}_h^n, w) \quad \forall n \geq 0.$$

Remark 4.1. Schemes (4.2) and (4.3), developed in [12], use standard Adams-Bashforth extrapolation for the explicit part, and a kind of modified Adams-Moulton interpolation which requires the coefficient at time step t^{n+1} to dominate the sum of the absolute values of the other coefficients. This extra requirement results in a stretched stencil. We consider this kind of IMEX schemes to ensure the unconditional stability.

4.2. Stability. In this subsection, we take the first order scheme (4.1) as an example, to investigate the stability of the IMEX-LDG methods for solving Oseen equations. The unconditional stability will be obtained for the velocity \mathbf{u}_h , the stress $\underline{\sigma}_h = \sqrt{\nu} \nabla \mathbf{u}_h$ and the pressure p_h . Although the stability results for the second and the third order schemes are a little different from the stability for the first order scheme, they can be obtained analogously. So we omit the proofs for higher order schemes to save space, we refer the readers to [17] for more details.

Theorem 4.1. *There exists a positive constant τ_0 independent of h , such that if $\tau \leq \tau_0$, then the solutions of scheme (4.1) satisfy*

$$(4.4) \quad \|\boldsymbol{u}_h^n\| \leq \|\boldsymbol{u}_h^0\|,$$

$$(4.5) \quad \|\underline{\sigma}_h^n\| \leq e^{C_0 n \tau} \|\underline{\sigma}_h^0\|,$$

$$(4.6) \quad \|p_h^n\| \leq C \left(\|\boldsymbol{u}_h^0\| + \frac{1}{\tau} \|\boldsymbol{u}_h^1 - \boldsymbol{u}_h^0\| + e^{C_0 n \tau} \|\underline{\sigma}_h^0\| \right),$$

where C_0 is a positive constant depending on $1/\sqrt{\nu}$, C is a positive constant independent of h and τ .

Proof.

Step 1 (prove (4.4)). Taking $\boldsymbol{v} = \boldsymbol{u}_h^{n+1}$, $\underline{r} = \tau \underline{\sigma}_h^{n+1}$, $w = \tau p_h^{n+1}$ in (4.1a), (4.1b) and (4.1c), respectively, and adding them together, we get

$$(4.7) \quad \underbrace{\frac{1}{2} \|\boldsymbol{u}_h^{n+1}\|^2 + \frac{1}{2} \|\boldsymbol{u}_h^{n+1} - \boldsymbol{u}_h^n\|^2 - \frac{1}{2} \|\boldsymbol{u}_h^n\|^2 + \tau \|\underline{\sigma}_h^{n+1}\|^2}_{LHS} = \underbrace{\tau \mathcal{H}(\boldsymbol{u}_h^n, \boldsymbol{u}_h^{n+1})}_{RHS},$$

where the LHS is obtained by applying Lemma 2.3 and the equality $(a - b)a = \frac{1}{2}[a^2 + (a - b)^2 - b^2]$ for arbitrary a, b . To bound the RHS , we write it as

$$RHS = \tau \mathcal{H}(\boldsymbol{u}_h^{n+1}, \boldsymbol{u}_h^{n+1}) - \tau \mathcal{H}(\boldsymbol{u}_h^{n+1} - \boldsymbol{u}_h^n, \boldsymbol{u}_h^{n+1}).$$

Hence, owing to Lemmas 2.1 and 2.4 we have

$$\begin{aligned} RHS &\leq C_\gamma \tau \|\boldsymbol{u}_h^{n+1} - \boldsymbol{u}_h^n\| (\|\nabla \boldsymbol{u}_h^{n+1}\| + \sqrt{\mu h^{-1}} \|\llbracket \boldsymbol{u}_h^{n+1} \rrbracket\|_{\Gamma_h}) \\ &\leq \frac{C_\gamma C_\mu}{\sqrt{\nu}} \tau \|\boldsymbol{u}_h^{n+1} - \boldsymbol{u}_h^n\| \|\underline{\sigma}_h^{n+1}\| \\ (4.8) \quad &\leq \tau \|\underline{\sigma}_h^{n+1}\|^2 + \frac{C_\gamma^2 C_\mu^2}{4\nu} \tau \|\boldsymbol{u}_h^{n+1} - \boldsymbol{u}_h^n\|^2, \end{aligned}$$

where Young's inequality is used in the last step. As a consequence, if we let $\frac{C_\gamma^2 C_\mu^2}{4\nu} \tau \leq \frac{1}{2}$, i.e., $\tau \leq \frac{2\nu}{C_\gamma^2 C_\mu^2}$, then

$$(4.9) \quad \|\boldsymbol{u}_h^{n+1}\| \leq \|\boldsymbol{u}_h^n\| \leq \cdots \leq \|\boldsymbol{u}_h^0\|.$$

Step 2 (prove (4.5)). Taking $\boldsymbol{v} = \boldsymbol{u}_h^{n+1} - \boldsymbol{u}_h^n$ in (4.1a), we get

$$\|\boldsymbol{u}_h^{n+1} - \boldsymbol{u}_h^n\|^2 = R_1 + R_2 + R_3,$$

where

$$\begin{aligned} R_1 &= \tau \mathcal{H}(\boldsymbol{u}_h^n, \boldsymbol{u}_h^{n+1} - \boldsymbol{u}_h^n) \\ &\leq C_\gamma \tau (\|\nabla \boldsymbol{u}_h^n\| + \sqrt{\mu h^{-1}} \|\llbracket \boldsymbol{u}_h^n \rrbracket\|_{\Gamma_h}) \|\boldsymbol{u}_h^{n+1} - \boldsymbol{u}_h^n\| \\ (4.10a) \quad &\leq \frac{C_\gamma C_\mu}{\sqrt{\nu}} \tau \|\underline{\sigma}_h^n\| \|\boldsymbol{u}_h^{n+1} - \boldsymbol{u}_h^n\| \leq \|\boldsymbol{u}_h^{n+1} - \boldsymbol{u}_h^n\|^2 + \frac{C_\gamma^2 C_\mu^2}{4\nu} \tau^2 \|\underline{\sigma}_h^n\|^2, \end{aligned}$$

$$\begin{aligned} R_2 &= \tau \mathcal{L}(\underline{\sigma}_h^{n+1}, \boldsymbol{u}_h^{n+1} - \boldsymbol{u}_h^n) = -\tau \mathcal{K}(\boldsymbol{u}_h^{n+1} - \boldsymbol{u}_h^n, \underline{\sigma}_h^{n+1}) \\ &= -\tau (\underline{\sigma}_h^{n+1} - \underline{\sigma}_h^n, \underline{\sigma}_h^{n+1}) \\ (4.10b) \quad &= -\frac{\tau}{2} \|\underline{\sigma}_h^{n+1}\|^2 - \frac{\tau}{2} \|\underline{\sigma}_h^{n+1} - \underline{\sigma}_h^n\|^2 + \frac{\tau}{2} \|\underline{\sigma}_h^n\|^2, \end{aligned}$$

$$(4.10c) \quad R_3 = \tau \mathcal{P}(p_h^{n+1}, \boldsymbol{u}_h^{n+1} - \boldsymbol{u}_h^n) = -\tau \mathcal{Q}(\boldsymbol{u}_h^{n+1} - \boldsymbol{u}_h^n, p_h^{n+1}) = 0.$$

In (4.10a) we used Lemmas 2.1 and 2.4, and Young's inequality; Lemma 2.3 and (4.1b), (4.1c) are used in (4.10b) and (4.10c). Thus,

$$(4.11) \quad \frac{\tau}{2} \|\underline{\sigma}_h^{n+1}\|^2 + \frac{\tau}{2} \|\underline{\sigma}_h^{n+1} - \underline{\sigma}_h^n\|^2 - \frac{\tau}{2} \|\underline{\sigma}_h^n\|^2 \leq \frac{C_\gamma^2 C_\mu^2}{4\nu} \tau^2 \|\underline{\sigma}_h^n\|^2.$$

The simple use of Gronwall's inequality leads to (4.5).

Step 3 (prove (4.6)). With the help of Lemma 2.5, we have, for $p_h^{n+1} \in L_0^2(\Omega)$, there exists $\mathbf{u}^* \in H_0^1(\Omega)^2$ such that $\|\mathbf{u}^*\|_1 \leq \alpha_2 \|p_h^{n+1}\|$ and

$$(4.12) \quad \|p_h^{n+1}\|^2 \leq C \underbrace{[\mathcal{K}(\mathbf{P}_h \mathbf{u}^*, \underline{\sigma}_h^{n+1}) + \mathcal{Q}(\mathbf{P}_h \mathbf{u}^*, p_h^{n+1})]}_S + \|\underline{\sigma}_h^{n+1}\|^2,$$

where we choose $r = \underline{\sigma}_h^{n+1}$ in (2.21). Again owing to Lemma 2.3 and (4.1a) we have

$$(4.13) \quad \begin{aligned} S &= -\mathcal{L}(\underline{\sigma}_h^{n+1}, \mathbf{P}_h \mathbf{u}^*) - \mathcal{P}(p_h^{n+1}, \mathbf{P}_h \mathbf{u}^*) \\ &= \mathcal{H}(\mathbf{u}_h^n, \mathbf{P}_h \mathbf{u}^*) - \frac{1}{\tau} (\mathbf{u}_h^{n+1} - \mathbf{u}_h^n, \mathbf{P}_h \mathbf{u}^*) = S_1 + S_2. \end{aligned}$$

From (2.12) we get

$$(4.14) \quad \begin{aligned} S_1 &\leq C_\gamma \|\mathbf{u}_h^n\| (\|\nabla \mathbf{P}_h \mathbf{u}^*\| + \sqrt{\mu h^{-1}} \|\llbracket \mathbf{P}_h \mathbf{u}^* \rrbracket\|_{\Gamma_h}) \\ &\leq C_\gamma \|\mathbf{u}_h^n\| (\|\mathbf{u}^*\|_1 + \sqrt{\mu h^{-1}} \|\llbracket \mathbf{u}^* - \mathbf{P}_h \mathbf{u}^* \rrbracket\|_{\Gamma_h}) \\ &\leq C \|\mathbf{u}_h^n\| \|\mathbf{u}^*\|_1 \leq C \alpha_2 \|\mathbf{u}_h^n\| \|p_h^{n+1}\|, \end{aligned}$$

where in the second line we used the property (2.19) and $\llbracket \mathbf{u}^* \rrbracket = 0$ across the element interface, the approximation property (2.18) is used in the third line. A simple application of the Cauchy-Schwarz inequality and (2.19) yields

$$(4.15) \quad S_2 \leq \frac{1}{\tau} \|\mathbf{u}_h^{n+1} - \mathbf{u}_h^n\| \|\mathbf{P}_h \mathbf{u}^*\| \leq \frac{C}{\tau} \|\mathbf{u}_h^{n+1} - \mathbf{u}_h^n\| \|\mathbf{u}^*\|_1 \leq \frac{C \alpha_2}{\tau} \|\mathbf{u}_h^{n+1} - \mathbf{u}_h^n\| \|p_h^{n+1}\|.$$

As a consequence

$$(4.16) \quad \|p_h^{n+1}\|^2 \leq C \left(\|\mathbf{u}_h^n\| + \frac{1}{\tau} \|\mathbf{u}_h^{n+1} - \mathbf{u}_h^n\| \right) \|p_h^{n+1}\| + C \|\underline{\sigma}_h^{n+1}\|^2.$$

Notice that we have proven $\|\mathbf{u}_h^n\| \leq \|\mathbf{u}_h^0\|$ in step 1, and we can also get

$$(4.17) \quad \|\mathbf{u}_h^{n+1} - \mathbf{u}_h^n\| \leq \|\mathbf{u}_h^1 - \mathbf{u}_h^0\|$$

using a similar procedure as for the proof for $\|\mathbf{u}_h^n\| \leq \|\mathbf{u}_h^0\|$, due to the linear structure of the scheme. Hence by applying Young's inequality to (4.16) we get

$$(4.18) \quad \|p_h^{n+1}\|^2 \leq C \left(\|\mathbf{u}_h^0\|^2 + \frac{1}{\tau^2} \|\mathbf{u}_h^1 - \mathbf{u}_h^0\|^2 + \|\underline{\sigma}_h^{n+1}\|^2 \right).$$

Thus we get (4.6) by using (4.5). \square

5. ERROR ESTIMATES

To derive the optimal error estimates for the IMEX-LDG schemes introduced in Subsection 4.1, we would like to resort to the Stokes projection, which has been studied in Section 3. To make the idea clear enough, we only take the first order scheme (4.1) as an example to present the outline of the proof.

To obtain the optimal error estimates for the first order scheme (4.1), we would like to assume the exact solution $\mathbf{u}(\mathbf{x}, t)$ and $p(\mathbf{x}, t)$ are smooth enough, for example,

$$(5.1a) \quad \mathbf{u}(\mathbf{x}, t) \in L^\infty(0, T; H^{k+2}(\Omega))^2, \quad p(\mathbf{x}, t) \in L^\infty(0, T; H^{k+2}(\Omega)),$$

and

$$(5.1b) \quad D_t^\ell \mathbf{u}(\mathbf{x}, t) \in L^\infty(0, T; H^{k+1}(\Omega))^2$$

for $\ell = 1, 2$, where $D_t^\ell \mathbf{u}$ means the ℓ th order time derivative of \mathbf{u} , and the notation $L^\infty(0, T; H^s(\Omega))$ represents the set of functions v such that

$$\max_{0 \leq t \leq T} \|v(\cdot, t)\|_{H^s(\Omega)} < \infty.$$

We give the main results in the following theorem.

Theorem 5.1. *Let $(\underline{\sigma}(\mathbf{x}, t), \mathbf{u}(\mathbf{x}, t), p(\mathbf{x}, t))$ be the exact solution of (2.1), satisfying the smoothness assumption (5.1), and let $(\underline{\sigma}_h^n, \mathbf{u}_h^n, p_h^n) \in \Sigma_h \times \mathbf{V}_h \times Q_h$ be the solution of the first order fully-discrete IMEX-LDG schemes (4.1). Then there exists a positive constant τ_0 independent of the spatial size h , such that if $\tau \leq \tau_0$, then*

$$(5.2) \quad \max_{n\tau \leq T} \{\|\mathbf{u}(\mathbf{x}, t^n) - \mathbf{u}_h^n\| + \|\underline{\sigma}(\mathbf{x}, t^n) - \underline{\sigma}_h^n\| + \|p(\mathbf{x}, t^n) - p_h^n\|\} \leq C(h^{k+1} + \tau),$$

where T is the final computing time and the bounding constant $C > 0$ is independent of h and τ .

We will prove Theorem 5.1 in the following two subsections.

5.1. Error division and error equation.

Denote

$$(\underline{\sigma}^n, \mathbf{u}^n, p^n) = (\underline{\sigma}(\mathbf{x}, t^n), \mathbf{u}(\mathbf{x}, t^n), p(\mathbf{x}, t^n)).$$

As the standard treatment in the finite element analysis, we decompose the error $\mathbf{e}^n = (\underline{e}_\sigma^n, \mathbf{e}_u^n, e_p^n) = (\underline{\sigma}^n - \underline{\sigma}_h^n, \mathbf{u}^n - \mathbf{u}_h^n, p^n - p_h^n)$ into two parts, namely, $\mathbf{e}^n = \boldsymbol{\xi}^n - \boldsymbol{\eta}^n$, where

$$(5.3) \quad \begin{aligned} \boldsymbol{\xi}^n &= (\underline{\xi}_\sigma^n, \boldsymbol{\xi}_u^n, \xi_p^n) = (\underline{\Pi}_h \underline{\sigma}^n - \underline{\sigma}_h^n, \boldsymbol{\Pi}_h \mathbf{u}^n - \mathbf{u}_h^n, \Pi_h p^n - p_h^n), \\ \boldsymbol{\eta}^n &= (\underline{\eta}_\sigma^n, \boldsymbol{\eta}_u^n, \eta_p^n) = (\underline{\Pi}_h \underline{\sigma}^n - \underline{\sigma}^n, \boldsymbol{\Pi}_h \mathbf{u}^n - \mathbf{u}^n, \Pi_h p^n - p^n), \end{aligned}$$

and $(\underline{\Pi}_h \underline{\sigma}^n, \boldsymbol{\Pi}_h \mathbf{u}^n, \Pi_h p^n)$ is the Stokes projection defined in (3.1).

Thanks to Lemma 3.2 and the linear structure of the Stokes projection, we have

$$(5.4a) \quad \|\boldsymbol{\eta}_u^n\| + \|\underline{\eta}_\sigma^n\| + \|\eta_p^n\| \leq Ch^{k+1},$$

$$(5.4b) \quad \|\boldsymbol{\eta}_u^{n+1} - \boldsymbol{\eta}_u^n\| \leq Ch^{k+1}\tau.$$

In what follows, we will focus on the estimate for $\boldsymbol{\xi}^n$. To this end, first we would like to establish the error equation. We can verify that the exact solution $(\underline{\sigma}^n, \mathbf{u}^n, p^n)$ satisfies

$$(5.5a) \quad (\mathbf{u}^{n+1}, \mathbf{v}) = (\mathbf{u}^n, \mathbf{v}) + \tau [\mathcal{H}(\mathbf{u}^n, \mathbf{v}) + \mathcal{L}(\underline{\sigma}^{n+1}, \mathbf{v}) + \mathcal{P}(p^{n+1}, \mathbf{v})] + (\boldsymbol{\zeta}^n, \mathbf{v}),$$

$$(5.5b) \quad (\underline{\sigma}^{n+1}, \underline{v}) = \mathcal{K}(\mathbf{u}^{n+1}, \underline{v}),$$

$$(5.5c) \quad 0 = \mathcal{Q}(\mathbf{u}^{n+1}, w),$$

with $\zeta^n = \mathcal{O}(\tau^2)$. Subtracting (4.1) from (5.5), and by the aid of the property of the Stokes projection (3.15), we get the error equation of ξ in the form

$$(5.6a) \quad (\xi_{\mathbf{u}}^{n+1} - \xi_{\mathbf{u}}^n, \mathbf{v}) = (\eta_{\mathbf{u}}^{n+1} - \eta_{\mathbf{u}}^n, \mathbf{v}) + \tau [\mathcal{H}(\mathbf{e}_{\mathbf{u}}^n, \mathbf{v}) + \mathcal{L}(\underline{\xi}_{\sigma}^{n+1}, \mathbf{v}) + \mathcal{P}(\xi_p^{n+1}, \mathbf{v})] + (\zeta^n, \mathbf{v}),$$

$$(5.6b) \quad (\underline{\xi}_{\sigma}^{n+1}, \underline{r}) = \mathcal{K}(\xi_{\mathbf{u}}^{n+1}, \underline{r}),$$

$$(5.6c) \quad 0 = \mathcal{Q}(\xi_{\mathbf{u}}^{n+1}, w).$$

5.2. Energy estimate for ξ . Even though the procedure to estimate ξ is similar to the stability analysis presented in Subsection 4.2, we would like to highlight the key technical ingredients. The first one is that we use the *Stokes projection* to eliminate the coupled impact of velocity error and pressure error, thus making the estimates clean and optimal. The second one is that by taking suitable test functions, we obtain the optimal error estimate for the stress variable, in $L^\infty(L^2)$ norm rather than in $L^2(L^2)$ norm. The third one is that the optimal error estimate for pressure depends on the optimal estimate for $\|\frac{\xi_{\mathbf{u}}^{n+1} - \xi_{\mathbf{u}}^n}{\tau}\|$, which needs to be considered carefully. Now we display the main conclusion in the following lemma.

Lemma 5.1. *There exists a positive constant τ_0 independent of the spatial size h , such that if $\tau \leq \tau_0$, then*

$$(5.7) \quad \|\xi_{\mathbf{u}}^n\| + \|\underline{\xi}_{\sigma}^n\| + \|\xi_p^n\| \leq C(h^{k+1} + \tau),$$

where C is independent of h and τ .

Proof.

Step 1 (estimate $\xi_{\mathbf{u}}$). Taking $(\mathbf{v}, \underline{r}, w) = (\xi_{\mathbf{u}}^{n+1}, \tau \underline{\xi}_{\sigma}^{n+1}, \tau \xi_p^{n+1})$ in (5.6) and adding them together, we have

$$(5.8) \quad \begin{aligned} & \frac{1}{2} \|\xi_{\mathbf{u}}^{n+1}\|^2 + \frac{1}{2} \|\xi_{\mathbf{u}}^{n+1} - \xi_{\mathbf{u}}^n\|^2 - \frac{1}{2} \|\xi_{\mathbf{u}}^n\|^2 + \tau \|\underline{\xi}_{\sigma}^{n+1}\|^2 \\ &= (\eta_{\mathbf{u}}^{n+1} - \eta_{\mathbf{u}}^n, \xi_{\mathbf{u}}^{n+1}) + \tau \mathcal{H}(\mathbf{e}_{\mathbf{u}}^n, \xi_{\mathbf{u}}^{n+1}) + (\zeta^n, \xi_{\mathbf{u}}^{n+1}) \doteq W_1 + W_2 + W_3, \end{aligned}$$

which is similar to (4.7). Owing to (2.12) we get

$$(5.9) \quad |W_2| \leq C_\gamma \tau \|\mathbf{e}_{\mathbf{u}}^n\| (\|\nabla \xi_{\mathbf{u}}^{n+1}\| + \sqrt{\mu h^{-1}} \|\llbracket \xi_{\mathbf{u}}^{n+1} \rrbracket\|_{\Gamma_h}).$$

Notice that the pair functions $(\xi_{\mathbf{u}}^{n+1}, \underline{\xi}_{\sigma}^{n+1})$ satisfy (5.6b), hence we get a similar result as for Lemma 2.4, i.e.,

$$(5.10) \quad \|\nabla \xi_{\mathbf{u}}^{n+1}\| + \sqrt{\mu h^{-1}} \|\llbracket \xi_{\mathbf{u}}^{n+1} \rrbracket\|_{\Gamma_h} \leq \frac{C_\mu}{\sqrt{\nu}} \|\underline{\xi}_{\sigma}^{n+1}\|.$$

Thus by the triangle inequality $\|\boldsymbol{e}_{\boldsymbol{u}}^n\| \leq \|\boldsymbol{\xi}_{\boldsymbol{u}}^n\| + \|\boldsymbol{\eta}_{\boldsymbol{u}}^n\|$, (5.4a) and Young's inequality we have

$$(5.11) \quad |W_2| \leq \frac{C_{\gamma} C_{\mu}}{\sqrt{\nu}} \tau (\|\boldsymbol{\xi}_{\boldsymbol{u}}^n\| + h^{k+1}) \|\underline{\boldsymbol{\xi}}_{\sigma}^{n+1}\| \leq \tau \|\underline{\boldsymbol{\xi}}_{\sigma}^{n+1}\|^2 + \frac{C_{\gamma}^2 C_{\mu}^2}{2\nu} \tau (\|\boldsymbol{\xi}_{\boldsymbol{u}}^n\|^2 + h^{2k+2}).$$

A simple use of the Cauchy-Schwarz inequality, the triangle inequality, (5.4b) and Young's inequality yields

$$(5.12) \quad \begin{aligned} |W_1 + W_3| &\leq \|\boldsymbol{\xi}_{\boldsymbol{u}}^{n+1}\| (\|\boldsymbol{\eta}_{\boldsymbol{u}}^{n+1} - \boldsymbol{\eta}_{\boldsymbol{u}}^n\| + \|\boldsymbol{\zeta}^n\|) \\ &\leq C(\|\boldsymbol{\xi}_{\boldsymbol{u}}^n\| + \|\boldsymbol{\xi}_{\boldsymbol{u}}^{n+1} - \boldsymbol{\xi}_{\boldsymbol{u}}^n\|)(h^{k+1}\tau + \tau^2) \\ &\leq \varepsilon \tau \|\boldsymbol{\xi}_{\boldsymbol{u}}^{n+1} - \boldsymbol{\xi}_{\boldsymbol{u}}^n\|^2 + C\tau \|\boldsymbol{\xi}_{\boldsymbol{u}}^n\|^2 + C(h^{2k+2}\tau + \tau^3). \end{aligned}$$

Consequently, if we choose ε small enough and let $\varepsilon\tau \leq 1$, we can get

$$(5.13) \quad \|\boldsymbol{\xi}_{\boldsymbol{u}}^{n+1}\|^2 - \|\boldsymbol{\xi}_{\boldsymbol{u}}^n\|^2 \leq C\tau \|\boldsymbol{\xi}_{\boldsymbol{u}}^n\|^2 + C(h^{2k+2} + \tau^2)\tau.$$

Then a simple application of the discrete Gronwall's inequality results in

$$(5.14) \quad \|\boldsymbol{\xi}_{\boldsymbol{u}}^n\| \leq C(h^{k+1} + \tau).$$

Step 2 (estimate $\underline{\boldsymbol{\xi}}_{\sigma}^n$). Taking $\boldsymbol{v} = \boldsymbol{\xi}_{\boldsymbol{u}}^{n+1} - \boldsymbol{\xi}_{\boldsymbol{u}}^n$ in (5.6a), and along a similar line as for the proof for (4.5), we get

$$\|\boldsymbol{\xi}_{\boldsymbol{u}}^{n+1} - \boldsymbol{\xi}_{\boldsymbol{u}}^n\|^2 = T_1 + T_2 + T_3 + T_4 + T_5,$$

where

$$\begin{aligned} T_1 &= \tau \mathcal{H}(\boldsymbol{\xi}_{\boldsymbol{u}}^n, \boldsymbol{\xi}_{\boldsymbol{u}}^{n+1} - \boldsymbol{\xi}_{\boldsymbol{u}}^n) \leq C_{\gamma} \tau (\|\nabla \boldsymbol{\xi}_{\boldsymbol{u}}^n\| + \sqrt{\mu h^{-1}} \|\llbracket \boldsymbol{\xi}_{\boldsymbol{u}}^n \rrbracket\|_{\Gamma_h}) \|\boldsymbol{\xi}_{\boldsymbol{u}}^{n+1} - \boldsymbol{\xi}_{\boldsymbol{u}}^n\|, \\ &\leq \frac{C_{\gamma} C_{\mu}}{\sqrt{\nu}} \tau \|\underline{\boldsymbol{\xi}}_{\sigma}^n\| \|\boldsymbol{\xi}_{\boldsymbol{u}}^{n+1} - \boldsymbol{\xi}_{\boldsymbol{u}}^n\| \leq \varepsilon \|\boldsymbol{\xi}_{\boldsymbol{u}}^{n+1} - \boldsymbol{\xi}_{\boldsymbol{u}}^n\|^2 + \frac{C_{\gamma}^2 C_{\mu}^2}{4\varepsilon\nu} \tau^2 \|\underline{\boldsymbol{\xi}}_{\sigma}^n\|^2, \\ T_2 &= \tau \mathcal{L}(\underline{\boldsymbol{\xi}}_{\sigma}^{n+1}, \boldsymbol{\xi}_{\boldsymbol{u}}^{n+1} - \boldsymbol{\xi}_{\boldsymbol{u}}^n) = -\tau \mathcal{K}(\boldsymbol{\xi}_{\boldsymbol{u}}^{n+1} - \boldsymbol{\xi}_{\boldsymbol{u}}^n, \underline{\boldsymbol{\xi}}_{\sigma}^{n+1}) = -\tau (\underline{\boldsymbol{\xi}}_{\sigma}^{n+1} - \underline{\boldsymbol{\xi}}_{\sigma}^n, \underline{\boldsymbol{\xi}}_{\sigma}^{n+1}) \\ &= -\frac{\tau}{2} \|\underline{\boldsymbol{\xi}}_{\sigma}^{n+1}\|^2 - \frac{\tau}{2} \|\underline{\boldsymbol{\xi}}_{\sigma}^{n+1} - \underline{\boldsymbol{\xi}}_{\sigma}^n\|^2 + \frac{\tau}{2} \|\underline{\boldsymbol{\xi}}_{\sigma}^n\|^2, \\ T_3 &= \tau \mathcal{P}(p_h^{n+1}, \boldsymbol{\xi}_{\boldsymbol{u}}^{n+1} - \boldsymbol{\xi}_{\boldsymbol{u}}^n) = -\tau \mathcal{Q}(\boldsymbol{\xi}_{\boldsymbol{u}}^{n+1} - \boldsymbol{\xi}_{\boldsymbol{u}}^n, p_h^{n+1}) = 0, \\ T_4 &= (\boldsymbol{\eta}_{\boldsymbol{u}}^{n+1} - \boldsymbol{\eta}_{\boldsymbol{u}}^n, \boldsymbol{\xi}_{\boldsymbol{u}}^{n+1} - \boldsymbol{\xi}_{\boldsymbol{u}}^n) + (\boldsymbol{\zeta}^n, \boldsymbol{\xi}_{\boldsymbol{u}}^{n+1} - \boldsymbol{\xi}_{\boldsymbol{u}}^n) \\ &\leq C(h^{k+1}\tau + \tau^2) \|\boldsymbol{\xi}_{\boldsymbol{u}}^{n+1} - \boldsymbol{\xi}_{\boldsymbol{u}}^n\| \leq \varepsilon \|\boldsymbol{\xi}_{\boldsymbol{u}}^{n+1} - \boldsymbol{\xi}_{\boldsymbol{u}}^n\|^2 + C(h^{2k+2}\tau^2 + \tau^4), \end{aligned}$$

and

$$(5.15) \quad T_5 = -\tau \mathcal{H}(\boldsymbol{\eta}_{\boldsymbol{u}}^n, \boldsymbol{\xi}_{\boldsymbol{u}}^{n+1} - \boldsymbol{\xi}_{\boldsymbol{u}}^n) \leq Ch^{k+1} \tau \|\boldsymbol{\xi}_{\boldsymbol{u}}^{n+1} - \boldsymbol{\xi}_{\boldsymbol{u}}^n\| \leq \varepsilon \|\boldsymbol{\xi}_{\boldsymbol{u}}^{n+1} - \boldsymbol{\xi}_{\boldsymbol{u}}^n\|^2 + Ch^{2k+2} \tau^2.$$

The estimate for T_5 is not trivial, to explain the details, we notice that

$$\begin{aligned}
 \mathcal{H}(\boldsymbol{\eta}_u, \mathbf{v}) &= \sum_K \int_K \boldsymbol{\gamma} \otimes \boldsymbol{\eta}_u : \nabla \mathbf{v} \, dx dy - \sum_e \int_e [\![\mathbf{v}]\!] \cdot \boldsymbol{\gamma} \otimes (\boldsymbol{\eta}_u)^- \cdot \mathbf{n}_e \, ds \\
 &= \sum_K \int_K \boldsymbol{\gamma} \otimes (\mathbf{u} - \boldsymbol{\pi}_h \mathbf{u}) : \nabla \mathbf{v} \, dx dy \\
 &\quad - \sum_e \int_e [\![\mathbf{v}]\!] \cdot \boldsymbol{\gamma} \otimes (\mathbf{u} - (\boldsymbol{\pi}_h \mathbf{u})^-) \cdot \mathbf{n}_e \, ds \\
 (5.16) \quad &+ \sum_K \int_K \boldsymbol{\gamma} \otimes \boldsymbol{\pi}_h \boldsymbol{\eta}_u : \nabla \mathbf{v} \, dx dy - \sum_e \int_e [\![\mathbf{v}]\!] \cdot \boldsymbol{\gamma} \otimes (\boldsymbol{\pi}_h \boldsymbol{\eta}_u)^- \cdot \mathbf{n}_e \, ds,
 \end{aligned}$$

for arbitrary $\mathbf{v} \in \mathbf{V}_h$, where \mathbf{n}_e is the outer normal of edge e which satisfies $\boldsymbol{\beta} \cdot \mathbf{n}_e < 0$, and $\boldsymbol{\beta} = (1, 1)^\top$ is defined before. Denote the first two terms and the last two terms on the right-hand side of the above equation as D_1 and D_2 , respectively. From the superconvergence property (3.14b), we have

$$(5.17) \quad |D_1| \leq Ch^{k+1} \|\mathbf{v}\|.$$

Integrating by parts we can get

$$(5.18) \quad D_2 = - \sum_K \int_K (\mathbf{v} \otimes \boldsymbol{\gamma}) : \nabla \boldsymbol{\pi}_h \boldsymbol{\eta}_u \, dx dy + \sum_e \int_e \mathbf{v} \cdot \boldsymbol{\gamma} \otimes [\![\boldsymbol{\pi}_h \boldsymbol{\eta}_u]\!] \cdot \mathbf{n}_e \, ds.$$

Thus by the aid of the Cauchy-Schwarz inequality and (3.28), (3.32) we have

$$\begin{aligned}
 |D_2| &\leq C_\gamma (\|\nabla \boldsymbol{\pi}_h \boldsymbol{\eta}_u\| + \sqrt{\mu h^{-1}} \|[\![\boldsymbol{\pi}_h \boldsymbol{\eta}_u]\!]\|_{\Gamma_h}) \|\mathbf{v}\| \\
 (5.19) \quad &\leq \frac{C_\gamma C_\mu}{\sqrt{\nu}} (h^{k+1} + \|\underline{\boldsymbol{\pi}_h \boldsymbol{\eta}_u}\|) \|\mathbf{v}\| \leq Ch^{k+1} \|\mathbf{v}\|.
 \end{aligned}$$

Consequently, the above estimates give rise to (5.15) by taking $\mathbf{v} = \xi_u^{n+1} - \xi_u^n$ and a simple application of Young's inequality.

Hence, choosing ε small enough and after simple algebraic manipulation, we have

$$(5.20) \quad \|\xi_\sigma^{n+1}\|^2 - \|\xi_\sigma^n\|^2 \leq C\tau \|\xi_\sigma^n\|^2 + C(h^{2k+2}\tau + \tau^3).$$

Thus, we get

$$(5.21) \quad \|\xi_\sigma^n\| \leq C(h^{k+1} + \tau)$$

directly by a simple use of the discrete Gronwall's inequality.

Step 3 (estimate ξ_p). From the stability analysis for p_h in Section 4, we see that, our estimate for p_h^{n+1} depends on $\frac{\mathbf{u}_h^{n+1} - \mathbf{u}_h^n}{\tau}$; see (4.16). Analogously, to estimate ξ_p we need the following lemma which states the estimate for $\frac{\xi_u^{n+1} - \xi_u^n}{\tau}$.

Lemma 5.2. *For arbitrary $n \geq 0$, there exists a positive constant τ_0 independent of h , such that if $\tau \leq \tau_0$, then*

$$(5.22) \quad \left\| \frac{\xi_u^{n+1} - \xi_u^n}{\tau} \right\| \leq C(h^{k+1} + \tau).$$

We will put the proof of this lemma in the Appendix. Now we are going to obtain the estimate for ξ_p . Thanks to Lemma 2.5, for $\xi_p^{n+1} \in L_0^2(\Omega)$, there exists $\mathbf{z}^* \in H_0^1(\Omega)^2$ such that $\|\mathbf{z}^*\|_1 \leq \alpha_2 \|\xi_p^{n+1}\|$ and

$$(5.23) \quad \|\xi_p^{n+1}\|^2 \leq C \underbrace{[\mathcal{K}(\mathbf{P}_h \mathbf{z}^*, \underline{\xi}_\sigma^{n+1}) + \mathcal{Q}(\mathbf{P}_h \mathbf{z}^*, \xi_p^{n+1}) + \|\underline{\xi}_\sigma^{n+1}\|^2]}_A,$$

where we choose $\underline{r} = \underline{\xi}_\sigma^{n+1}$ in (2.21). By Lemma 2.3 and (5.6a), we get

$$\begin{aligned} A &= -\mathcal{L}(\underline{\xi}_\sigma^{n+1}, \mathbf{P}_h \mathbf{z}^*) - \mathcal{P}(\xi_p^{n+1}, \mathbf{P}_h \mathbf{z}^*) \\ &= -\left(\frac{\xi_u^{n+1} - \xi_u^n}{\tau}, \mathbf{P}_h \mathbf{z}^*\right) + \left(\frac{\eta_u^{n+1} - \eta_u^n}{\tau}, \mathbf{P}_h \mathbf{z}^*\right) \\ &\quad + \left(\frac{\zeta^n}{\tau}, \mathbf{P}_h \mathbf{z}^*\right) + \mathcal{H}(e_u^n, \mathbf{P}_h \mathbf{z}^*) \\ (5.24) \quad &= A_1 + A_2 + A_3 + A_4. \end{aligned}$$

A simple use of the Cauchy-Schwarz inequality gives rise to

$$\begin{aligned} |A_1 + A_2 + A_3| &\leq \left(\left\| \frac{\xi_u^{n+1} - \xi_u^n}{\tau} \right\| + \left\| \frac{\eta_u^{n+1} - \eta_u^n}{\tau} \right\| + \left\| \frac{\zeta^n}{\tau} \right\| \right) \|\mathbf{P}_h \mathbf{z}^*\| \\ &\leq C(h^{k+1} + \tau) \|\mathbf{z}^*\|_1 \leq C(h^{k+1} + \tau) \|\xi_p^{n+1}\| \\ (5.25) \quad &\leq \varepsilon \|\xi_p^{n+1}\|^2 + C(h^{2k+2} + \tau^2), \end{aligned}$$

where we have used Lemma 5.2, (5.4b), and (2.19) in the second line, and Young's inequality in the third line. Proceeding with a similar procedure as for (4.14), we get

$$\begin{aligned} |A_4| &\leq C(\|\xi_u^n\| + \|\eta_u^n\|)(\|\nabla \mathbf{P}_h \mathbf{z}^*\| + \sqrt{\mu h^{-1}} \|\llbracket \mathbf{P}_h \mathbf{z}^* \rrbracket\|_{\Gamma_h}) \\ &\leq C(h^{k+1} + \tau)(\|\mathbf{z}^*\|_1 + \sqrt{\mu h^{-1}} \|\llbracket \mathbf{z}^* - \mathbf{P}_h \mathbf{z}^* \rrbracket\|_{\Gamma_h}) \\ &\leq C(h^{k+1} + \tau) \|\mathbf{z}^*\|_1 \leq C\alpha_2(h^{k+1} + \tau) \|\xi_p^{n+1}\| \\ (5.26) \quad &\leq \varepsilon \|\xi_p^{n+1}\|^2 + C(h^{2k+2} + \tau^2), \end{aligned}$$

for arbitrary $\varepsilon > 0$. As a consequence, choosing ε small enough, and combining the above estimates, we have

$$(5.27) \quad \|\xi_p^{n+1}\|^2 \leq C(h^{2k+2} + \tau^2 + \|\underline{\xi}_\sigma^{n+1}\|^2).$$

Then it follows straightforwardly by using the result of (5.21) that

$$(5.28) \quad \|\xi_p^n\| \leq C(h^{k+1} + \tau).$$

Combining the above estimates we complete the proof of this lemma. \square

Finally, we get (5.2) by Lemma 5.1, (5.4a), and the triangle inequality, thus complete the proof of Theorem 5.1.

6. NUMERICAL EXPERIMENTS

In this section, we will numerically validate the error accuracy of the fully-discrete IMEX-LDG schemes introduced in Section 4, for solving the time-dependent Oseen equation (1.1) and the Navier-Stokes equation

$$(6.1) \quad \begin{cases} \frac{\partial \mathbf{u}}{\partial t} - \nu \Delta \mathbf{u} + \nabla \cdot (\mathbf{u} \otimes \mathbf{u}) + \nabla p = \mathbf{0}, \\ \nabla \cdot \mathbf{u} = 0, \\ \mathbf{u}(\mathbf{x}, 0) = \mathbf{u}^0(\mathbf{x}), \end{cases}$$

on $(x, y) \in [-\pi, \pi] \times [-\pi, \pi]$. We consider the following three examples, for the first two we adopt periodic boundary conditions.

Example 1. The Oseen equation (1.1) with $\gamma = (1, 1)^\top$, the source term $\mathbf{f} = (0, -2e^{-2\nu t} \cos(x+y))^\top$, and the exact solution

$$\mathbf{u}(x, y, t) = \begin{pmatrix} e^{-2\nu t} \sin x \cos y \\ -e^{-2\nu t} \cos x \sin y \end{pmatrix}, \quad p(x, y, t) = -e^{-2\nu t} \sin(x+y).$$

Example 2. The Navier-Stokes equation (6.1) with the exact solution

$$\mathbf{u}(x, y, t) = \begin{pmatrix} e^{-2\nu t} \sin x \cos y \\ -e^{-2\nu t} \cos x \sin y \end{pmatrix}, \quad p(x, y, t) = \frac{1}{4}e^{-4\nu t}(\cos(2x) + \cos(2y)).$$

Example 3. The Navier-Stokes equation (6.1) in $[0, \pi] \times [0, \pi]$ with the same exact solution as in Example 2, but the boundary condition for \mathbf{u} is given by the exact solution taken values at the boundary, which is nonperiodic.

Remark 6.1. For the Oseen equation (1.1) and Navier-Stokes equation (6.1) with Dirichlet boundary condition

$$(6.2) \quad \mathbf{u}|_{\partial\Omega} = \mathbf{u}_b(\mathbf{x}, t),$$

the numerical flux (2.6) should be modified by

$$(6.3) \quad \begin{aligned} \widehat{\mathbf{u}_{h,\sigma}}|_e &= \begin{cases} \mathbf{u}_h^-, & e \subset \Gamma_h^i, \\ \mathbf{u}_b, & e \subset \Gamma_h^b, \end{cases} \\ \widehat{\underline{\sigma}_h}|_e &= \begin{cases} \underline{\sigma}_h^+, & e \subset \Gamma_h \setminus \partial\Omega^+, \\ \underline{\sigma}_h^- - \frac{\delta_1}{h}(\mathbf{u}_h^- - \mathbf{u}_b) \otimes \mathbf{n}_e, & e \subset \partial\Omega^+, \end{cases} \\ \widehat{\mathbf{u}_{h,p}}|_e &= \begin{cases} \mathbf{u}_h^- - \delta_2 [\![p_h]\!], & e \subset \Gamma_h^i, \\ \mathbf{u}_b, & e \subset \Gamma_h^b, \end{cases} \\ \widehat{p_h}|_e &= \begin{cases} p_h^+, & e \subset \Gamma_h \setminus \partial\Omega^+, \\ p_h^-, & e \subset \partial\Omega^+, \end{cases} \end{aligned}$$

where Γ_h^i and Γ_h^b represents the set of all interior edges and boundary edges, respectively. The unit normal vector \mathbf{n}_e points outward on the boundary edge e , and $\delta_1, \delta_2 > 0$ are penalty parameters. It can be proved that the scheme is still stable, and the corresponding *Stokes projection* can be defined and analyzed. We will give the definition of the corresponding Stokes projection in the Appendix, and prove that it is well-defined. Additional work is required for the error estimates for non-periodic boundary conditions, which will be left for future work.

For all the examples, we will test for $\nu = 1, 0.1, 0.01$ and 0.001 , on uniform rectangular meshes. The final computing time is $T = 1$ in all the experiments. We use Q_0 , Q_1 , and Q_2 elements for schemes (4.1), (4.2), and (4.3), respectively. We plot the L^2 errors for the velocity $\|\mathbf{u} - \mathbf{u}_h\|$, the stress $\|\boldsymbol{\sigma} - \boldsymbol{\sigma}_h\|$ and the pressure $\|p - p_h\|$ versus the number of partitions n in the x and y directions in a log-log scale in Figures 1–3, for different viscosity constants ν . The time step taken in each test is listed in Table 1. The numerical flux in the convection part is chosen as the upwind numerical flux for Example 1, and as the simple central flux for Example 2 and Example 3, to avoid possible order reduction due to the change of wind directions. In addition, for Example 3, we take the penalty parameters $\delta_1 = 10$ and $\delta_2 = 0.1$ in each test.

TABLE 1. The time step taken in the experiments.

		Example 1				Example 2				Example 3			
ν		1	0.1	0.01	0.001	1	0.1	0.01	0.001	1	0.1	0.01	0.001
scheme		h	h	h	$0.5h$	$0.5h$	$0.5h$	$0.1h$	h	h	h	h	
(4.1)		h	h	h	$0.5h$	$0.5h$	$0.5h$	$0.1h$	h	h	h	h	
(4.2)		h	h	h	$0.1h$	$0.5h$	$0.5h$	$0.1h$	$0.1h$	$0.1h$	$0.1h$	$0.1h$	
(4.3)		$0.1h$	$0.1h$	$0.1h$	$0.1h$	$0.1h$	$0.1h$	$0.05h$	$0.05h$	$0.1h$	$0.1h$	$0.05h$	$0.05h$

From Figure 1, we observe the optimal error accuracy for velocity, stress and pressure of the three schemes, for different viscosity constant ν . From Figure 2, we can also observe the optimal error accuracy except the stress in the last picture (in the case $\nu = 0.001$ for the third order scheme (4.3)), which is about 2.7. So we can conclude that for periodic boundary problems, the schemes can achieve optimal order of accuracy in $L^\infty(L^2)$ norm for velocity, stress and pressure. The error of stress may depend on $1/\sqrt{\nu}$. From Figure 3, we observe the optimal error accuracy for velocity in each test. The order of accuracy for stress and pressure are almost optimal for the first order scheme (4.1). For scheme (4.2), we observe optimal order of accuracy for pressure, but about half order lower for stress. For scheme (4.3), about half order is lost for stress and almost optimal error is achieved for pressure.

Finally, we test for the flow in a confined cavity $[0, 1] \times [0, 1]$ with boundary conditions $(u, v) = (1, 0)$ on the top, $(u, v) = (0, -1)$ on the right, $(u, v) = (-1, 0)$ on the bottom and $(u, v) = (0, 1)$ on the left. We display the streamlines and contours of pressure for $\nu = 0.001$ on 80×80 uniform rectangle grids in Figure 4, where we use Q_1 element as the spatial discretization and the first order time marching scheme (4.1), the computing time is $T = 1$ and the time step is $\tau = 0.1h$. In this experiment, the penalty parameters are taken as $\delta_1 = 10$ and $\delta_2 = 0.1$.

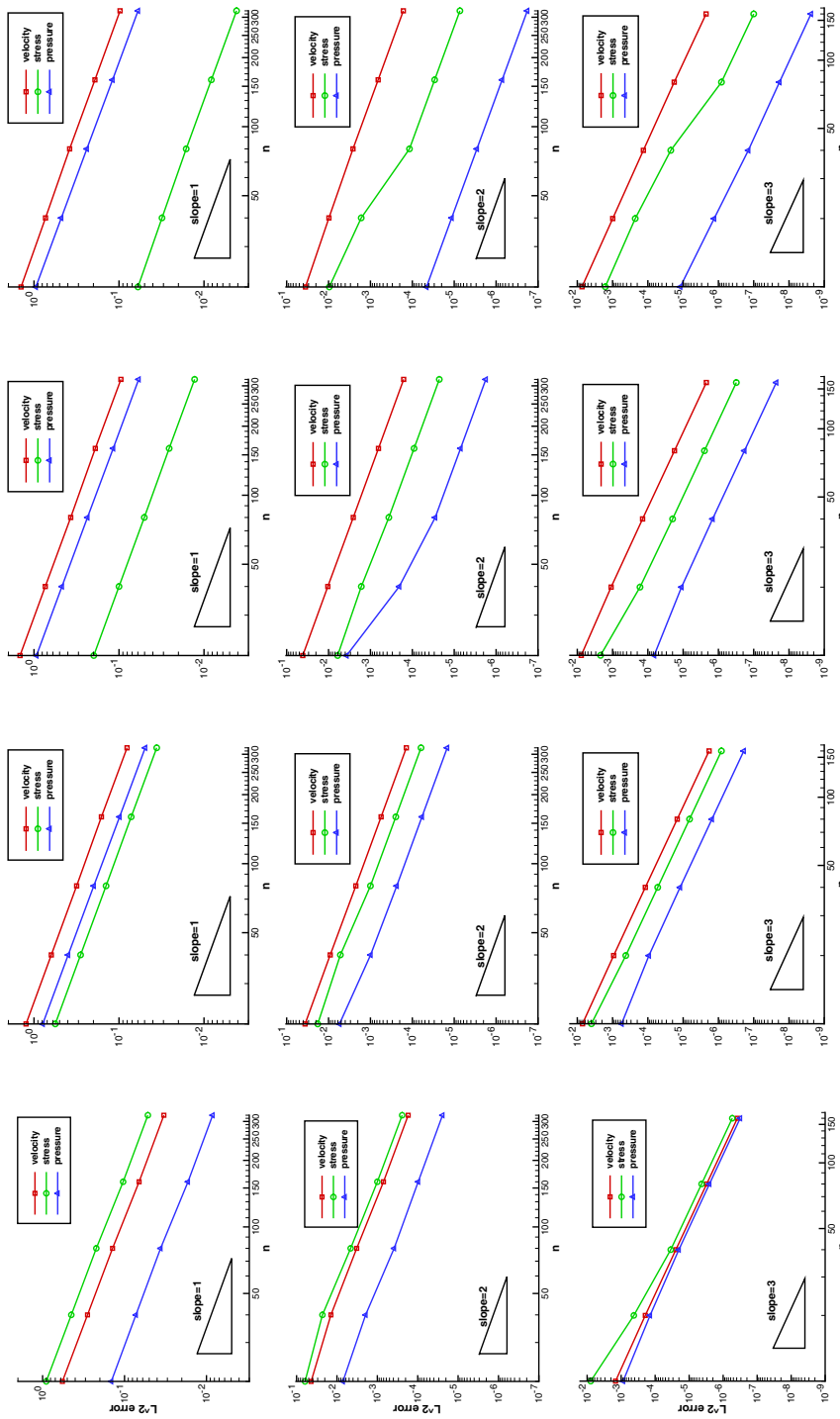


FIGURE 1. L^2 errors for velocity, stress and pressure for Example 1. From the top to bottom are schemes (4.1), (4.2), and (4.3), respectively, and in each row, from the left to right, $\nu = 1, 0.1, 0.01, 0.001$, respectively.

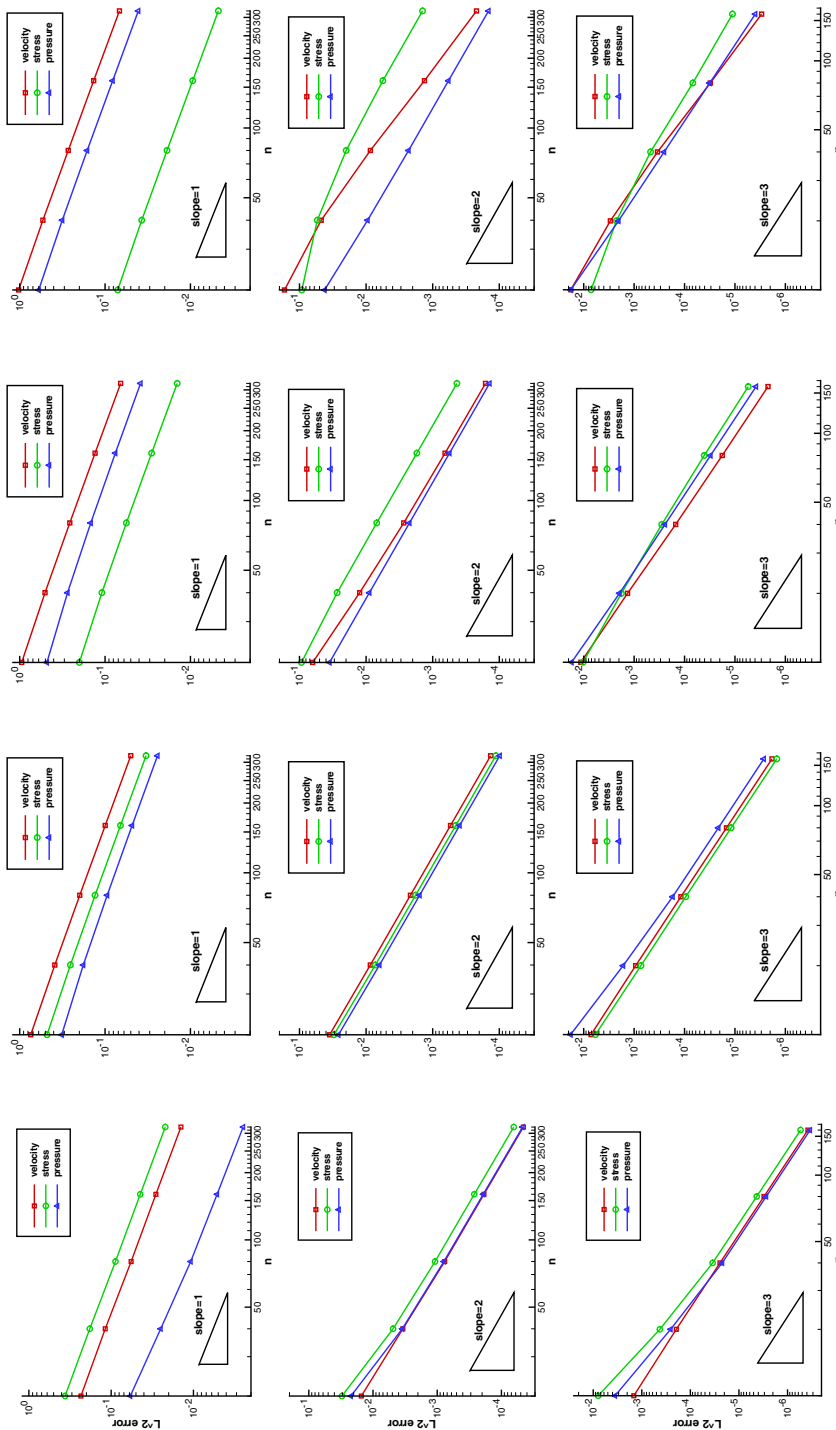


FIGURE 2. L^2 errors for velocity, stress and pressure for Example 2. From the top to bottom are schemes (4.1), (4.2), and (4.3), respectively, and in each row, from the left to right, $\nu = 1, 0.1, 0.01, 0.001$, respectively.

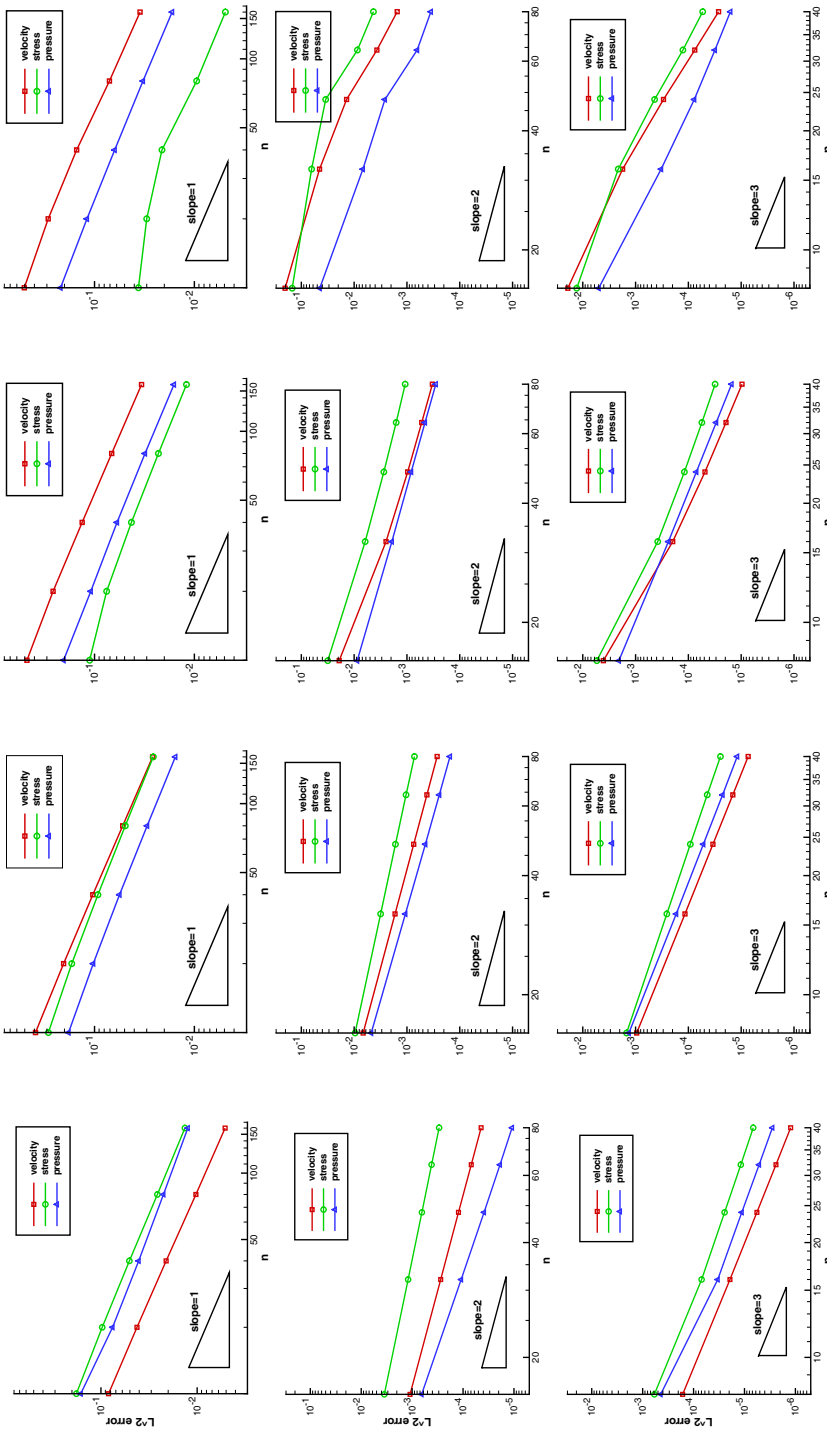


FIGURE 3. L^2 errors for velocity, stress and pressure for Example 3. From the top to bottom are schemes (4.1), (4.2), and (4.3), respectively, and in each row, from the left to right, $\nu = 1, 0.1, 0.01, 0.001$, respectively.

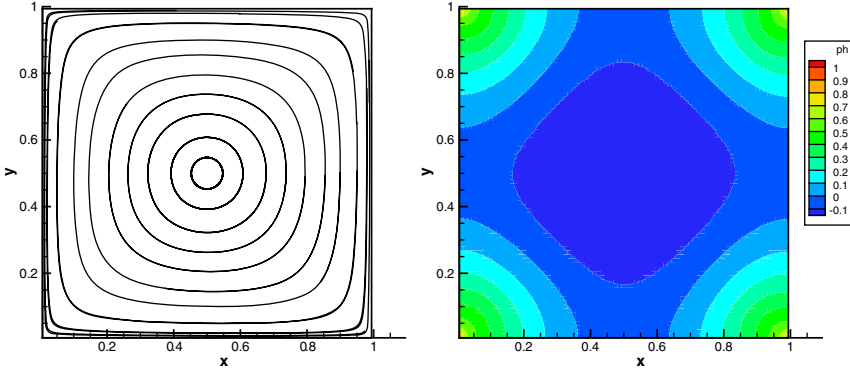


FIGURE 4. Streamlines (left) and contours of pressure (right) for $\nu = 0.001$.

7. CONCLUDING REMARKS

We have studied IMEX time marching methods coupled with the LDG schemes for solving two-dimensional unsteady incompressible Oseen equation with periodic boundary conditions. We showed that the first order IMEX-LDG scheme is unconditionally stable for the Oseen equations, in the sense that the time-step τ is only required to be bounded from above by a positive constant independent of the spatial mesh size h . Furthermore, by the aid of the so-called *Stokes projection* and the *inf-sup* argument, we obtain optimal error estimates for all the three variables, i.e., the velocity, the stress and the pressure, all in $L^\infty(L^2)$ norm. Numerical examples are given to verify our main results, not only for the first order scheme, but also for two specific multi-step IMEX-LDG schemes of second and third order, as well as for the Navier-Stokes equations. However, for high order multi-step schemes, the optimal error estimate for pressure is not available in our framework of analysis, which constitutes our future work. Our schemes also work for nonperiodic boundary conditions, stability of the schemes can be proved, and the corresponding Stokes projection can be well-defined. However, careful study on suitable numerical fluxes at the boundary and other boundary treatment techniques are necessary to ensure optimal error accuracy, which will be left for our future work. Our next goal also includes the corresponding study for the Navier-Stokes equations, where the treatment for the nonlinear term would require further work.

8. APPENDIX

Proof of Lemma 5.2. First, we claim that the lemma holds true for $n = 0$, i.e.,

$$(8.1) \quad \|\xi_{\mathbf{u}}^1 - \xi_{\mathbf{u}}^0\| \leq C(h^{k+1}\tau + \tau^2).$$

We would like to skip the proof of (8.1) at present, and continue to prove Lemma 5.2 for general n . From (5.6), we can get

$$(8.2a) \quad (\xi_{\mathbf{u}}^n - \xi_{\mathbf{u}}^{n-1}, \mathbf{v}) = (\eta_{\mathbf{u}}^n - \eta_{\mathbf{u}}^{n-1}, \mathbf{v}) + \tau[\mathcal{H}(\mathbf{e}_{\mathbf{u}}^{n-1}, \mathbf{v}) + \mathcal{L}(\underline{\xi}_{\sigma}^n, \mathbf{v}) + \mathcal{P}(\xi_p^n, \mathbf{v})] \\ + (\zeta^{n-1}, \mathbf{v}),$$

$$(8.2b) \quad (\underline{\xi}_{\sigma}^n, \underline{r}) = \mathcal{K}(\xi_{\mathbf{u}}^n, \underline{r}),$$

$$(8.2c) \quad 0 = \mathcal{Q}(\xi_{\mathbf{u}}^n, w).$$

Subtracting (8.2) from (5.6), we get

$$(8.3a) \quad (\xi_u^{n+1} - \xi_u^n, v) = (\xi_u^n - \xi_u^{n-1}, v) + (\eta_u^{n+1} - 2\eta_u^n + \eta_u^{n-1}, v) + (\zeta^n - \zeta^{n-1}, v) \\ + \tau[\mathcal{H}(e_u^n - e_u^{n-1}, v) + \mathcal{L}(\underline{\xi}_\sigma^{n+1} - \underline{\xi}_\sigma^n, v) + \mathcal{P}(\xi_p^{n+1} - \xi_p^n, v)],$$

$$(8.3b) \quad (\underline{\xi}_\sigma^{n+1} - \underline{\xi}_\sigma^n, \underline{r}) = \mathcal{K}(\xi_u^{n+1} - \xi_u^n, \underline{r}),$$

$$(8.3c) \quad 0 = \mathcal{Q}(\xi_u^{n+1} - \xi_u^n, w).$$

Taking $(v, \underline{r}, w) = (\xi_u^{n+1} - \xi_u^n, \tau(\underline{\xi}_\sigma^{n+1} - \underline{\xi}_\sigma^n), \tau(\xi_p^{n+1} - \xi_p^n))$ in (8.3), and adding them together, we obtain

$$(8.4) \quad \frac{1}{2}\|\xi_u^{n+1} - \xi_u^n\|^2 + \frac{1}{2}\|\xi_u^{n+1} - 2\xi_u^n + \xi_u^{n-1}\|^2 - \frac{1}{2}\|\xi_u^n - \xi_u^{n-1}\|^2 + \tau\|\underline{\xi}_\sigma^{n+1} - \underline{\xi}_\sigma^n\|^2 = \mathcal{T}_c + \mathcal{T}_p,$$

where

$$(8.5) \quad \mathcal{T}_c = \tau\mathcal{H}(e_u^n - e_u^{n-1}, \xi_u^{n+1} - \xi_u^n),$$

$$(8.6) \quad \mathcal{T}_p = (\eta_u^{n+1} - 2\eta_u^n + \eta_u^{n-1}, \xi_u^{n+1} - \xi_u^n) + (\zeta^n - \zeta^{n-1}, \xi_u^{n+1} - \xi_u^n).$$

Owing to (2.12) and the triangle inequality, we can easily get

$$(8.7) \quad \begin{aligned} \mathcal{T}_c &\leq C_\gamma\tau(\|\xi_u^n - \xi_u^{n-1}\| + \|\eta_u^n - \eta_u^{n-1}\|) \\ &\quad \times \|\nabla(\xi_u^{n+1} - \xi_u^n)\| + \sqrt{\mu h^{-1}}\|\xi_u^{n+1} - \xi_u^n\|_{\Gamma_h} \\ &\leq \frac{C_\gamma C_\mu}{\sqrt{\nu}}\tau(\|\xi_u^n - \xi_u^{n-1}\| + h^{k+1}\tau)\|\underline{\xi}_\sigma^{n+1} - \underline{\xi}_\sigma^n\| \\ &\leq \tau\|\underline{\xi}_\sigma^{n+1} - \underline{\xi}_\sigma^n\|^2 + C\tau\|\xi_u^n - \xi_u^{n-1}\|^2 + Ch^{2k+2}\tau^3, \end{aligned}$$

where (5.4b) and Lemma 2.4 are used in the second inequality, and Young's inequality is used in the last inequality.

Moreover, it can be proved that $\|\eta_u^{n+1} - 2\eta_u^n + \eta_u^{n-1}\| \leq Ch^{k+1}\tau^2$ and $\zeta^n - \zeta^{n-1} = \mathcal{O}(\tau^3)$. Hence

$$(8.8) \quad \begin{aligned} |\mathcal{T}_p| &\leq C(h^{k+1}\tau^2 + \tau^3)\|\xi_u^{n+1} - \xi_u^n\| \leq C\tau\|\xi_u^{n+1} - \xi_u^n\|^2 + C\tau(h^{2k+2}\tau^2 + \tau^4) \\ &\leq C\tau\|\xi_u^n - \xi_u^{n-1}\|^2 + C\tau\|\xi_u^{n+1} - 2\xi_u^n + \xi_u^{n-1}\|^2 + C\tau(h^{2k+2}\tau^2 + \tau^4). \end{aligned}$$

Thus, from (8.4), (8.7) and (8.8), we obtain

$$(8.9) \quad \|\xi_u^{n+1} - \xi_u^n\|^2 - \|\xi_u^n - \xi_u^{n-1}\|^2 \leq C\tau\|\xi_u^n - \xi_u^{n-1}\|^2 + C\tau(h^{2k+2}\tau^2 + \tau^4),$$

if $C\tau \leq \frac{1}{2}$. So the simple use of the discrete Gronwall's inequality and (8.1) yields

$$(8.10) \quad \|\xi_u^{n+1} - \xi_u^n\| \leq C(h^{k+1}\tau + \tau^2).$$

Before we complete the proof of Lemma 5.2, we should show (8.1). Assume $\mathbf{u}_h^0 = \mathbf{\Pi}_h \mathbf{u}^0$, where $\mathbf{\Pi}_h$ is the Stokes projection defined in (3.1), so $\xi_u^0 = 0$. Hence it suffices to show $\|\xi_u^1\| \leq C(h^{k+1}\tau + \tau^2)$. Consider $n = 1$ in (8.2) and taking $v = \xi_u^1$, we get

$$(8.11) \quad \|\xi_u^1\|^2 + \tau\|\underline{\xi}_\sigma^1\|^2 = \underbrace{(\eta_u^1 - \eta_u^0, \xi_u^1)}_{\mathcal{V}_p} + \underbrace{(\zeta^0, \xi_u^1)}_{\mathcal{V}_c} + \underbrace{\tau\mathcal{H}(e_u^0, \xi_u^1)}_{\mathcal{V}_c}.$$

Notice that $\|\eta_u^1 - \eta_u^0\| \leq Ch^{k+1}\tau$ and $\|\zeta^0\| \leq C\tau^2$. So due to the Cauchy-Schwarz inequality and Young's inequality, we get

$$(8.12) \quad \mathcal{V}_p \leq \varepsilon\|\xi_u^1\|^2 + C_\varepsilon(h^{k+1}\tau + \tau^2)^2.$$

Thanks to the bilinear structure of the operator $\mathcal{H}(\cdot, \cdot)$, we have

$$\mathcal{H}(\mathbf{e}_u^0, \mathbf{v}) = \mathcal{H}(\boldsymbol{\xi}_u^0, \mathbf{v}) - \mathcal{H}(\boldsymbol{\eta}_u^0, \mathbf{v}) = -\mathcal{H}(\boldsymbol{\eta}_u^0, \mathbf{v}),$$

so along the same line as the estimate for T_5 in (5.15) we get

$$(8.13) \quad |\mathcal{V}_c| \leq Ch^{k+1}\tau \|\boldsymbol{\xi}_u^1\| \leq \varepsilon \|\boldsymbol{\xi}_u^1\|^2 + C_\varepsilon(h^{k+1}\tau)^2,$$

for arbitrary ε . Finally, from (8.11), (8.12), and (8.13) we derive

$$(8.14) \quad \|\boldsymbol{\xi}_u^1\| \leq C(h^{k+1}\tau + \tau^2)$$

by choosing ε small enough. Up to now, we have completed the proof of Lemma 5.2. \square

The Stokes projection for the Dirichlet boundary condition. For the convenience of expression, we denote the corresponding operators $\mathcal{L}, \mathcal{K}, \mathcal{P}, \mathcal{Q}$ for the Dirichlet boundary conditions with the numerical fluxes (6.3) as $\tilde{\mathcal{L}}, \tilde{\mathcal{K}}, \tilde{\mathcal{P}}, \tilde{\mathcal{Q}}$, respectively.

The Stokes projection for the Dirichlet boundary condition problem is defined as

$$(8.15a) \quad \tilde{\mathcal{L}}(\underline{\Pi}_h \underline{\sigma}, \mathbf{v}) + \tilde{\mathcal{P}}(\Pi_h p, \mathbf{v}) = \tilde{\mathcal{L}}(\underline{\sigma}, \mathbf{v}) + \tilde{\mathcal{P}}(p, \mathbf{v}),$$

$$(8.15b) \quad (\underline{\Pi}_h \underline{\sigma}, \underline{r}) = \tilde{\mathcal{K}}(\Pi_h \mathbf{u}, \underline{r}),$$

$$(8.15c) \quad \tilde{\mathcal{Q}}(\Pi_h \mathbf{u}, w) = \tilde{\mathcal{Q}}(\mathbf{u}, w),$$

and

$$(8.15d) \quad \int_{\Omega} (\Pi_h p - p) \, dx dy = 0.$$

We conclude that the projection defined in (8.15) is also well-defined. To prove it, we assume the exact solution $(\underline{\sigma}, \mathbf{u}, p) = (\underline{0}, \mathbf{0}, 0)$ and the boundary condition $\mathbf{u}_b = \mathbf{0}$. Taking $(\underline{r}, \mathbf{v}, w) = (\underline{\Pi}_h \underline{\sigma}, \Pi_h \mathbf{u}, \Pi_h p)$ in (8.15) and adding them together leads to

$$\|\underline{\Pi}_h \underline{\sigma}\|^2 + \frac{\delta_1}{h} \sum_{e \in \partial\Omega^+} \int_e (\Pi_h \mathbf{u}^- \cdot \mathbf{n}_e)^2 \, ds + \delta_2 \sum_{e \in \Gamma_h^i} \int_e [\Pi_h p]^2 \, ds = 0$$

which implies $\underline{\Pi}_h \underline{\sigma} = \underline{0}$, $\Pi_h \mathbf{u}^- \cdot \mathbf{n} = 0$ on $\partial\Omega^+$ and $[\Pi_h p] = 0$ at the interior element interfaces. Next taking $\underline{r} = \Pi_h \mathbf{u} \otimes \beta$ in (8.15b) we get

$$\frac{1}{2} \sum_{e \in \Gamma_h^i} \int_e [\Pi_h \mathbf{u}] \cdot [\Pi_h \mathbf{u}] (\beta \cdot \mathbf{n}_e) + \frac{1}{2} \sum_{e \in \partial\Omega^+} (\Pi_h \mathbf{u}^- \cdot \mathbf{n}_e)^2 - \frac{1}{2} \sum_{e \in \partial\Omega^-} (\Pi_h \mathbf{u}^+ \cdot \mathbf{n}_e)^2 = 0,$$

where $\beta \cdot \mathbf{n}_e < 0$. Thus $\Pi_h \mathbf{u}^+ \cdot \mathbf{n} = 0$ on $\partial\Omega^-$ and $[\Pi_h \mathbf{u}] = \mathbf{0}$ at the interior element interfaces, since $\Pi_h \mathbf{u}^- \cdot \mathbf{n} = 0$ on $\partial\Omega^+$. Then we can get $\nabla \Pi_h \mathbf{u} = \underline{0}$ in each element K , along a similar argument as for (3.5). Hence we prove that $\Pi_h \mathbf{u} = \mathbf{0}$.

Since $\underline{\Pi}_h \underline{\sigma} = \underline{0}$, from (8.15a) we have

$$0 = \tilde{\mathcal{P}}(\Pi_h p, \mathbf{v}) = - \sum_{K \in \Omega_h} \int_K \nabla \Pi_h p \cdot \mathbf{v} \, dx dy - \sum_{e \in \Gamma_h^i} [\Pi_h p] \mathbf{v}^- \cdot \mathbf{n}_e \, ds.$$

Noting that $[\Pi_h p] = 0$ at the interior element interfaces, we take $\mathbf{v} = \nabla \Pi_h p$ to get $\nabla \Pi_h p = \mathbf{0}$ in each element K , thus $\Pi_h p$ is continuous and is a constant in Ω . Owing to the condition (8.15d) we get $\Pi_h p = 0$.

REFERENCES

- [1] U. M. Ascher, S. J. Ruuth, and R. J. Spiteri, *Implicit-explicit Runge-Kutta methods for time-dependent partial differential equations*, Appl. Numer. Math. **25** (1997), no. 2-3, 151–167, DOI 10.1016/S0168-9274(97)00056-1. MR1485812
- [2] F. Bassi and S. Rebay, *A high-order accurate discontinuous finite element method for the numerical solution of the compressible Navier-Stokes equations*, J. Comput. Phys. **131** (1997), no. 2, 267–279, DOI 10.1006/jcph.1996.5572. MR1433934
- [3] A. Cesmelioglu, B. Cockburn, N. C. Nguyen, and J. Peraire, *Analysis of HDG methods for Oseen equations*, J. Sci. Comput. **55** (2013), no. 2, 392–431, DOI 10.1007/s10915-012-9639-y. MR3044180
- [4] P. G. Ciarlet, *The Finite Element Method for Elliptic Problems*, Studies in Mathematics and its Applications, Vol. 4, North-Holland Publishing Co., Amsterdam-New York-Oxford, 1978. MR0520174
- [5] B. Cockburn, G. Kanschat, I. Perugia, and D. Schötzau, *Superconvergence of the local discontinuous Galerkin method for elliptic problems on Cartesian grids*, SIAM J. Numer. Anal. **39** (2001), no. 1, 264–285, DOI 10.1137/S0036142900371544. MR1860725
- [6] B. Cockburn, G. Kanschat, and D. Schötzau, *The local discontinuous Galerkin method for the Oseen equations*, Math. Comp. **73** (2004), no. 246, 569–593, DOI 10.1090/S0025-5718-03-01552-7. MR2031395
- [7] B. Cockburn, G. Kanschat, D. Schötzau, and C. Schwab, *Local discontinuous Galerkin methods for the Stokes system*, SIAM J. Numer. Anal. **40** (2002), no. 1, 319–343, DOI 10.1137/S0036142900380121. MR1921922
- [8] B. Cockburn, G. Kanschat, and D. Schotzau, *A locally conservative LDG method for the incompressible Navier-Stokes equations*, Math. Comp. **74** (2005), no. 251, 1067–1095, DOI 10.1090/S0025-5718-04-01718-1. MR2136994
- [9] B. Cockburn and C.-W. Shu, *The local discontinuous Galerkin method for time-dependent convection-diffusion systems*, SIAM J. Numer. Anal. **35** (1998), no. 6, 2440–2463, DOI 10.1137/S0036142997316712. MR1655854
- [10] B. Cockburn and C.-W. Shu, *Runge-Kutta discontinuous Galerkin methods for convection-dominated problems*, J. Sci. Comput. **16** (2001), no. 3, 173–261, DOI 10.1023/A:1012873910884. MR1873283
- [11] V. Girault and P.-A. Raviart, *Finite Element Methods for Navier-Stokes Equations: Theory and Algorithms*, Springer Series in Computational Mathematics, vol. 5, Springer-Verlag, Berlin, 1986. MR851383
- [12] S. Gottlieb and C. Wang, *Stability and convergence analysis of fully discrete Fourier collocation spectral method for 3-D viscous Burgers' equation*, J. Sci. Comput. **53** (2012), no. 1, 102–128, DOI 10.1007/s10915-012-9621-8. MR2965307
- [13] E. Hairer and G. Wanner, *Solving Ordinary Differential Equations. II: Stiff and Differential-Algebraic Problems*, 2nd ed., Springer Series in Computational Mathematics, vol. 14, Springer-Verlag, Berlin, 1996. MR1439506
- [14] Y. Liu and C.-W. Shu, *Analysis of the local discontinuous Galerkin method for the drift-diffusion model of semiconductor devices*, Sci. China Math. **59** (2016), no. 1, 115–140, DOI 10.1007/s11425-015-5055-8. MR3436999
- [15] X. Meng, C.-W. Shu, and B. Wu, *Optimal error estimates for discontinuous Galerkin methods based on upwind-biased fluxes for linear hyperbolic equations*, Math. Comp. **85** (2016), no. 299, 1225–1261, DOI 10.1090/mcom/3022. MR3454363
- [16] H. Wang, C.-W. Shu, and Q. Zhang, *Stability and error estimates of local discontinuous Galerkin methods with implicit-explicit time-marching for advection-diffusion problems*, SIAM J. Numer. Anal. **53** (2015), no. 1, 206–227, DOI 10.1137/140956750. MR3296621
- [17] H. Wang, C.-W. Shu, and Q. Zhang, *Stability analysis and error estimates of local discontinuous Galerkin methods with implicit-explicit time-marching for nonlinear convection-diffusion problems. part 2*, Appl. Math. Comput. **272** (2016), no. part 2, 237–258, DOI 10.1016/j.amc.2015.02.067. MR3421105
- [18] H. Wang, S. Wang, Q. Zhang, and C.-W. Shu, *Local discontinuous Galerkin methods with implicit-explicit time-marching for multi-dimensional convection-diffusion problems*, ESAIM Math. Model. Numer. Anal. **50** (2016), no. 4, 1083–1105, DOI 10.1051/m2an/2015068. MR3521713

- [19] S. Wang, W. Deng, J. Yuan, and Y. Wu, *Characteristic local discontinuous Galerkin methods for incompressible Navier-Stokes equations*, Commun. Comput. Phys. **22** (2017), no. 1, 202–227, DOI 10.4208/cicp.220515.031016a. MR3673548

COLLEGE OF SCIENCE, NANJING UNIVERSITY OF POSTS AND TELECOMMUNICATIONS, NANJING 210023, JIANGSU PROVINCE, PEOPLE'S REPUBLIC OF CHINA
Email address: hjwang@njupt.edu.cn

SCHOOL OF MATHEMATICS, SHANDONG UNIVERSITY, JINAN 250100, SHANDONG PROVINCE, PEOPLE'S REPUBLIC OF CHINA
Email address: xliu@sdu.edu.cn

DEPARTMENT OF MATHEMATICS, NANJING UNIVERSITY, NANJING 210093, JIANGSU PROVINCE, PEOPLE'S REPUBLIC OF CHINA
Email address: qzh@nju.edu.cn

DIVISION OF APPLIED MATHEMATICS, BROWN UNIVERSITY, PROVIDENCE, RHODE ISLAND 02912
Email address: shu@dam.brown.edu